6

NEUTRON ACTIVATION ANALYSIS USING AN ^{241}Am-Be NEUTRON SOURCE

by

Egigu Tequash

A Thesis

Submitted in Partial Fulfillement for the Requirements

for the Degree Master of Science in Physics

in the Addis Ababa University

June, 1995

Addis Ababa, Ethiopia

DEDICATION

To my father Tequash Alemu who has
dedicated for the education of his children
and could see only flowers, but not lucky
enough to see the fruits.

ACKNOWLEDGEMENTS

I am greatly indebted to my advisor Dr. Siegfried Tesch for his generous advice, devoted assistance, in all stages of the work, constant guidance and constructive criticism which were necessary for the progress of the project.

I would like to express my best gratitude to Dr. Wang Dahai, from IAEA, for his continuos encouragement and indirect involvement in this work during his stay in Addis Ababa.

I am thankful to Ato Mengistalem Mebrate for his co-operation in providing me constantly the liquid nitrogen for the experiment. The Radiation Protection Authority is acknowledged for allowing me to use their facilities at my initial working stage. Lastly I wish to express my thanks to all my instructors in the Department of Physics of Addis Ababa University and the Department of Physics as whole.

TABLE OF CONTENTS

ABSTRACT

The purpose of this work is to explore the possibility of using an isotopic neutron source for neutron activation analysis (NAA) for the first time at Addis Ababa University. An americium- beryllium neutron source was used to develop a method for activation analysis of copper in brass. Element analysis was completed by identifying copper and then determining the concentration of copper in brass by comparative method. Neutron activation analysis of I, Ni and Mn has been carried out , and the results are also discussed.

INTRODUCTION

One of the great achievements of nuclear physics is the discovery of the phenomena of artificial radioactivity which plays a major role for activation analysis. After the discovery of induced, or artificial radioactivity by Curie and Juliot in 1933, its application to the solution of analytical problems was readily recognised in 1936. Heavesy and Levi used thermal neutrons to determine the concentration of dysprosium impurities in yttrium[1]. The increasing application of radionuclides and nuclear chemistry to analytical problems led to a rapid growth of activation analysis as an established laboratory technique by the time of the 1955 International Conference on Peaceful Uses of Atomic Energy. Neutron Activation Analysis (NAA) is defined as a nuclear method of elemental analysis, in which one or more elements in the sample to be analysed are made radioactive by bombardment with suitable nuclear particles and the induced radioactive species are then identified and measured quantitatively. Neutron activation analysis has earned a reputation as being one of the most sensitive and reliable methods for trace element determination in a wide variety of materials. Neutron activation analysis useful to measure physical properties of materials, such as the segregation of trace impurities in metals, the homogeneity of charcoal and to the study diverse fields as archaeology, biology e.t.c. Activation analysis has been also used to determine the efficiency of special purification steps for high-purity metals [1].

It is necessary here to point out that elemental composition of soils may be of interest not only in the prospecting of ore deposits but also in recording possible changes in the environment due to man's activities. During the development of mineral resources local and regional contamination of the environment may occur and some of the contaminating elements may be of public health significance, contamination may occur near smelters and

may also result from urban industrial activity. As the world becomes more and more to an industrial economy, surveillance of environmental changes becomes imperative. Neutron activation analysis is likely to become one of the most effective means of surveillance of changes in trace element composition of soils, water and air [2].

The installation of the necessary equipment for neutron activation analysis in the Physics Department of the Addis Ababa University is of great advantage for Ethiopia to use the NAA method for practical applications and research work. With this in mind, as a starting point the work is intended to use NAA method for the qualitative identification of iodine, manganese, nickel and the investigation of copper in brass. Furthermore, we try to obtain accurate measurements of the concentration of copper-64 radionuclide in brass samples. The chemical composition of brass was determined by neutron activation analysis (NAA) via activation of copper which is the main part of brass, using both short and long term irradiation of brass and standard copper samples with thermal neutrons from Am-Be neutron source and subsequent gamma spectrometry with a germanium detector. The same technique was applied when investigating chemical compounds and nickel.

The first chapter deals with the interaction of particles and radiation with matter, these encompasses the photoelectric effect, the Compton effect and the pair-formation properties of gamma-ray interaction.The working principle of detectors, especially the properties of Ge detectors are described in chapter 2. In chapter 3 and 4 the main physical features of NAA, and the experimental equipment and methods used in the experiment are discussed. The measured data of chapter 5 are treated using a comparative counting method to determine the half-life and amount of copper in brass and the qualitative identification of iodine, manganese and nickel respectively.

1. INTERACTION OF PARTICLES AND RADIATION WITH MATTER

When particles pass through matter, they interact with the atoms constituting the substance, i.e. with electrons and atomic nuclei. Depending on the type the particles they can participate in strong, electromagnetic or weak interaction.

Table 1.1 Particles and radiation which take part in strong , electromagnetic or weak interaction

particles/ Radiation	Strong interaction	Electromagnetic interaction	Weak interaction
Neutrons	X	X	X[a]
Protons	X	X	-
Electron/ Positron	-	X	X[b]
Gamma- ray	-	X	-

X[a] . neutrons decay weakly but does interact weakly.

X[b], electron/ positron appear in β-decay

We describe in detail the main types of interaction of neutron and γ-quanta with matter (photoelectric effect, Compton effect, and formation of electron-positron pairs) in chapter (1.1) and (1.2) as these processes are essential for the understanding of γ-spectra measured with Ge detectors.

1.1. INTERACTION OF NEUTRONS WITH MATTER

The behaviour of neutrons in matter is quite different from that of either charged particles or gamma rays. Since the neutrons are uncharged, no Coulomb forces come into play with

either the atomic electrons or the nuclei. Thus, for neutrons to interact with matter, they must either enter the nucleus or come sufficiently close to it for the nuclear forces to act. For the interaction of the neutron with electromagnetic field of atoms the magnetic moment of the neutron is essential. The capture reaction of a neutron with a nucleus ${}_{Z}X^{A}$ can be written as

$$ {}_{Z}X^{A} + {}_{0}n^{1} \Rightarrow ({}_{Z}X^{A+1})^{*} \qquad (1\text{-}1) $$

where $({}_{Z}X^{A+1})^{*}$ represents the compound nucleus in an excited state. The excitation energy, including both the binding energy and the kinetic energy of the neutron, is distributed among the constituents of the nucleus. The compound nucleus remains in the excited state only a short time, about 10^{-20} s. The excitation energy may be removed by the emission of one or several particles.

Processes in which the neutron is re-emitted are referred to as scattering compound process. The scattering can be inelastic or elastic, depending on whether the nucleus is left in an excited or the ground state after the neutron re-emission. In *elastic scattering*, the neutron collides with the target nucleus and bounces off it similar to the collision of two billiard balls. During the collision, the neutron loses some energy. All of this transferred energy appears as kinetic energy of the target nucleus. Light elements are best for slowing down neutrons by elastic scattering, so materials with a high hydrogen content (such as paraffin, water) are used. In *inelastic scattering* the incoming neutrons impart some of their energy to the scattering material and excite the target nucleus. This nucleus usually emits gamma radiation when returning to the ground state. The inelastic scattering process is most important for heavy nuclei [4]. As the neutron energy in the interaction with matter is important, a classification of neutrons according to their energies is useful. Thermal neutrons are those which have reached thermal equilibrium with their surroundings. At 20^{0}C

thermal neutrons have an average kinetic energy of 0.025 eV. Epithermal neutrons are the group between thermal and fast. The lower boundary on the fast-neutron group is quite arbitrary-perhaps about 100 keV is a convenient value.

1.2. INTERACTION OF GAMMA RADIATION WITH MATTER

Gamma rays interact with matter mainly by one of the three competing processes illustrated in Fig.1.1 These are the photoelectric effect, Compton scattering and pair production, respectively.

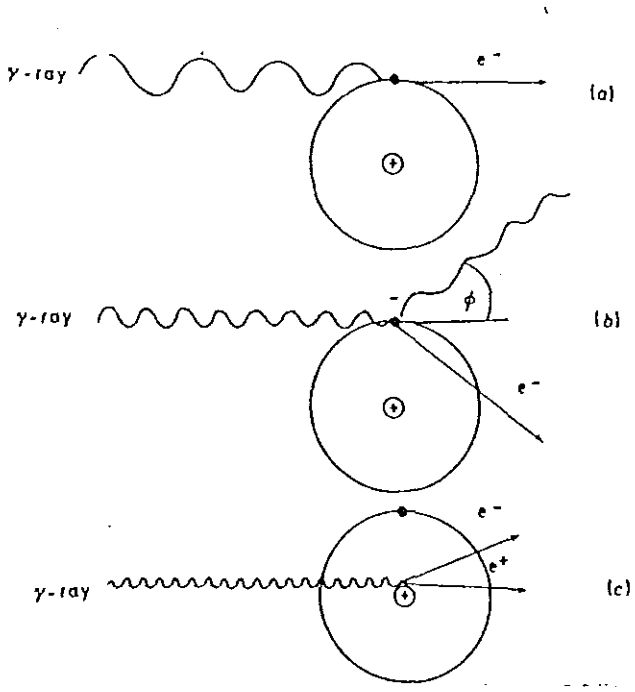

Fig. 1.1 Interaction of gamma rays . a) Photoelectric effect b) Compton scattering c) Pair production [5].

The interaction of the gamma ray with matter is largely determined by the energy of the gamma ray and the electron density or atomic number of the material. Fig 1.2 shows the energy dependence of the absorption cross-sections for gamma-quanta in lead for each of the three interaction mechanisms. We shall describe here the main types of interaction of gamma radiation with matter.

1.2.1. PHOTOELECTRIC EFFECT

The photoelectric effect is the process of interaction of a γ-quantum with an electron attached to an atom, during which the entire energy of the γ–quantum is transferred to the electron. As a result of this interaction, the electron is ejected from the atom with a kinetic energy

$$T_e = E_\gamma - I_i \qquad (1\text{-}2)$$

where E_γ is the energy of the γ-quantum and I_i is the ionisation potential of the i^{th} atomic shell. In order to fulfill the conservation of momentum and energy, the photoelectric effect cannot take place on a free electron, it is possible only for bound electrons.

The photoelectric effect is especially significant for materials of heavy elements where the probability of interaction is considerable. In low-Z materials, this effect becomes significant only for low energies of γ–rays. The specific nature of photoelectric absorption is employed for measuring the gamma radiation. Proportional detectors for gamma spectrometry use the photoelectric effect to produce an output pulse which is proportional to the energy of the gamma ray. The photoelectric effect predominates at energies below 400 keV.

1.2.2. COMPTON EFFECT

The interaction of gamma-rays with matter may result in its scattering, i.e. manifests itself in the deviation from its initial direction of propagation by a certain angle . Instead of giving up its entire energy to the electron, the photon transfers only a part of its energy to an electron, which in this case may be either bound or free [6]. The energy loss of the scattered photon varies with the scattering angle. It is at maximum when it is back-scattered at 180 degrees and is a minimum when the scattering angle is zero degrees. Compton scattering can take

place several times, within a large detector, until the energy is extinguished. Typical regions of the γ–spectrum consists Compton edge energy and backscatter peak.

1.2.3. ELECTRON-POSITRON PAIR FORMATION

For γ–quanta having a very high energy, there exists another form of interaction of γ–quanta with matter besides the photoelectric and the Compton effect, viz. the formation of electron-positron pairs. Pair production is not an important mode of interaction below 1.5 MeV but at energies larger than 5 MeV it is the predominant mechanism comparable to Compton scattering (see Fig. 1.2). The created positron will soon collide with an electron and the reverse process of annihilation will take place producing two gamma rays of energy 511 keV . If the pair formation takes place in the Coulomb field of a nucleus the energy of the recoil nucleus will be quite low and hence the threshold energy E_0 of the γ–quantum , required for the creation of a pair, practically coincides with twice the rest mass of the electron:

$$E_0 = 2m_e c^2 = 1.02 \text{ MeV}$$

The cross-section of electron-positron pair formation in the Coulomb field of an electron is much (about 1000 times) smaller than the cross-section of their formation in the field of a nucleus [7].

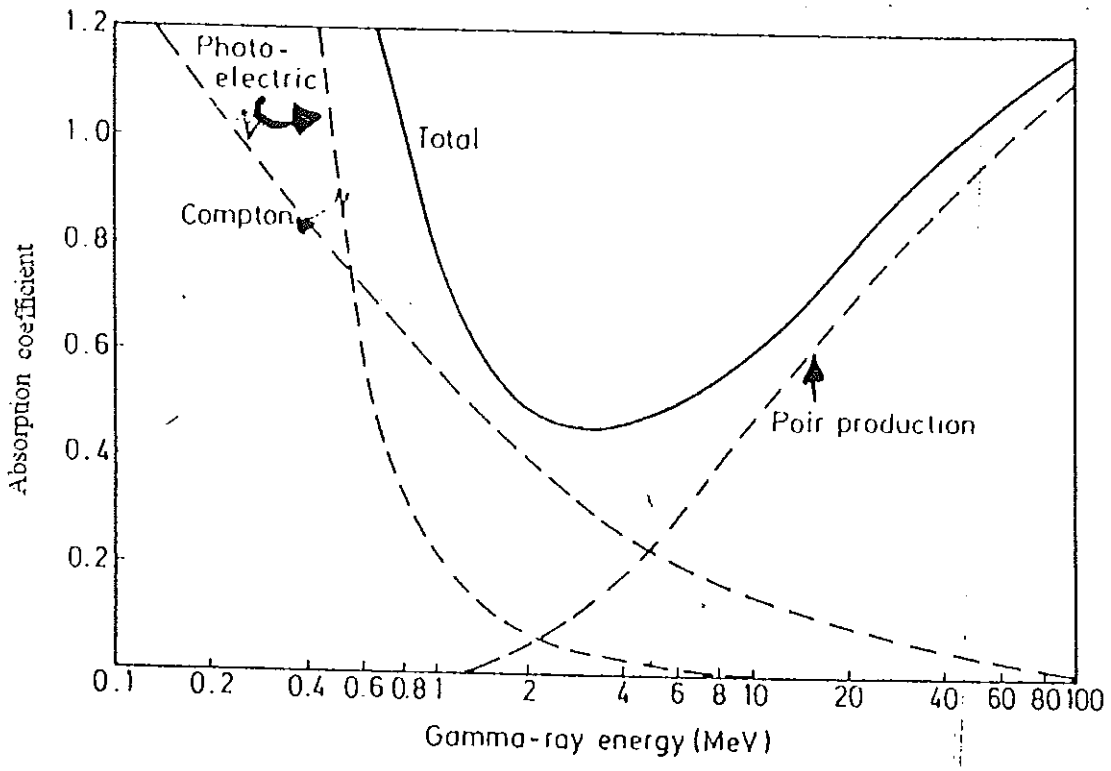

Fig. 1.2 Gamma-ray absorption coefficient in lead [5].

2. RADIATION DETECTORS

In the preceding chapter we saw that the principal interactions of radiation with matter result in the production of charge carriers with a reduction in energy of the radiation. The uncharged neutron is detected only indirectly, through recoil protons (from fast neutrons) or through nuclear transmutations or induced radioactivity (from fast or slow neutrons).

An instrument for the detection and measurement of radiation generally consists of two parts: a detector which converts the energy of the radiation into an electrical pulse, and an electronic circuit which amplifies and records the pulses produced [8].

A) SEMICONDUCTOR DETECTORS

Semiconductor detectors are essentially solid ionisation chambers. The ionisation produced by radiation in a semiconductor crystal is collected as an electrical pulse, amplified, and counted by suitable quantifying device. One major advantage of the semiconductor is the much higher density of the medium, giving the detector a greater nuclear radiation stopping power compared to other types of detectors. A semiconductor detector can completely stop the radiation to obtain a complete energy transfer to the detector. Another important property of the semiconductor detector is its higher energy resolution. Semiconductor detectors are commonly used in radiation spectrometry owing to their superior energy resolution capability for electromagnetic radiation.

Semiconductor materials like silicon and germanium in certain forms can be used as radiation detectors. The electrical conductivity of a material depends upon the number of electrons which are free to move, within the material under the influence of an applied

potential difference. In semiconductors most of the electrons are fixed, as in insulators, but a small amount of impurity can render the material conductive.

When an n-type semiconductor is made with a region of p-type atom we have a p-n junction diode. The electrons are free to move from n-type to p-type, that is from the region of electron excess to the region of electron deficiency. Thus a p-n junction will allow a current to flow in one direction. The n-type and p-type regions represent the electrodes on either side of the intrinsic region, which is electrically neutral . The detector is always reverse biased so that it does not conduct. When gamma rays enter the intrinsic region, which is shown like in Fig. 2.1, they may interact by liberating electrons. The primary liberated electrons produce secondary electrons which are free to move and can be collected by the positive electrode. The number of electrons collected is proportional to the energy given up by the gamma ray.

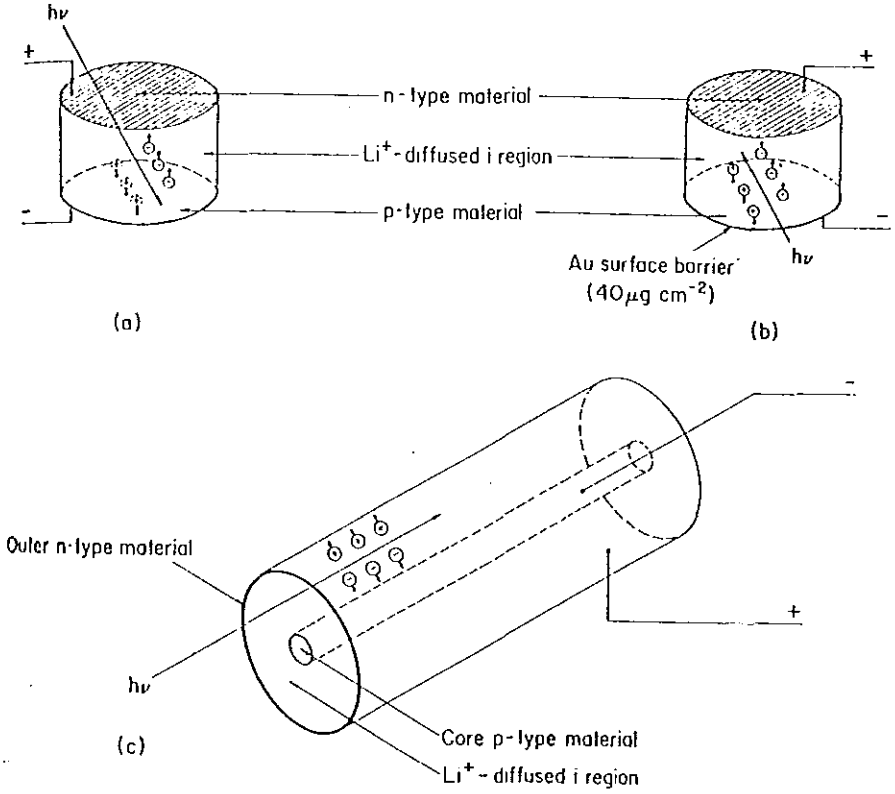

Fig. 2.2 Basic types of p-i-n compensated Ge(Li) detector devices. A path of incident radiation, hv, is illustrated along with the directions of electrons, O. and holes, O, produced within the detector [10]

B) GERMANIUM DETECTORS

The operation of photon detector generally involves sequentially [19]

- conversion of photon energy to kinetic energy of electrons(and positrons) by photoelectric absorption, Compton scattering or pair production.
- the production of electron-ion pairs, electron-hole pairs or excited molecular states by these electron.
- the collection and measurement of the light emitted in the de-excitation of the molecular states.

The ability of a detector to measure photons is characterised by the peak width and the detection efficiency for the corresponding gamma energy. The width is commonly specified as the FWHM in keV, also called resolution. The efficiency of the detector is the ratio of the number of counts in the peak corresponding to the absorption of all the photon energy to the number of photons of that energy emitted by the sourc e. Both the peak width and the peak efficiency are functions of the photon energy.

The density of the detector material, its atomic number and its volume is important for the conversion of photon energy to kinetic energy of electrons. The detector which is used in this work is a coaxial germanium detector.

a. DETECTOR MOUNTING

The Ge detector assembly has the following parts:

- cooling system
- high-quality vacuum around the detector crystal
- mounting for the electrical contacts and
- thin entrance window .

b. DETECTOR COOLING normally is achieved mounting the detector on one end of a metal rod, while the other end protrudes into the tank of liquid nitrogen. Liquid nitrogen, which has a temperature of 77^{0}K, is the common cooling medium for germanium detectors. The detector is mounted in a vacuum chamber which is attached to or inserted into a liquid nitrogen dewar. The sensitive detector is thus protected from moisture and condensable contaminants. The liquid nitrogen cryostat is one of the most important component in assuring reliable long term performance of a Ge-detector system. The type of cryostat used here is a dip stick type, which has vertical orientation, and a capacity of 30 litres.

C. *HIGH-QUALITY VACUUM* is necessary to minimise the collection of contaminants on the detector surfaces which cause degradation of the performance. The first stage of the preamplifier is also mounted in the vacuum. The detector is thermally shielded to prevent the heat from the outer surfaces to the detector. The vacuum acts as a shield against conductive and convective heat transfer, and reflective materials are used to minimize radiation loss.

3. CONCEPTS OF NEUTRON ACTIVATION ANALYSIS

Neutron activation analysis is specific because the radioactivity induced can be characterised by half-lives of the radionuclides produced and by the radiation emitted. The decay rates and radiation energies are never exactly duplicate in any other radioisotope produced by neutron irradiation [11]. Thus an exact knowledge of their nuclear characteristics allows to determine the element present.

The rate of formation of a particular activation product, R_F , in a given sample is proportional to the intensity of the flux of incident neutrons, to the concentration of the target nuclide in the sample, and to the cross-section for the nuclear reaction. Thus for the case of neutron irradiation it holds

$$R_F = \phi \sigma n = \frac{\phi}{A} \sigma m f N^0 \qquad (3.1)$$

where

ϕ is the neutron flux

σ is the reaction cross-section

n is the number of target atoms

m is the mass of the trace element in the specimen

f is the fractional isotopic abundance of the target nuclide

A is the atomic weight of the trace element

N^0 is Avogadro number

The decay rate, D, expressed in atomic disintegrations per second, of the product radionuclide in the specimen is given by

$$D = n\lambda \tag{3.2}$$

where

n is the number of the atoms of the nuclide in specimen

λ is the decay constant of the nuclide

Therefore, the rate of change of the quantity of the activation product during irradiation is given by

$$\frac{dN}{dt} = R_F - D = \frac{\phi}{A}\sigma m f N^0 - n\lambda \tag{3.3}$$

The disintegration rate of the radionuclide in the specimen after an arbitrary irradiation time T is

$$D(t) = \frac{\phi}{A}\sigma m f N^0 (1 - \exp(-\lambda T)) \tag{3.4}$$

For sufficiently long irradiation time exp(-λT) approaches zero, so that Equ. (3.4) becomes

$$D^{\infty} = \frac{\phi}{A}\sigma m f N^0 \tag{3.5}$$

Eq. (3.4) can also be written in the following form for calculating the sensitivity for detection of an element under specified set of irradiation and detection condition

$$m = \frac{AD(t)}{\phi\sigma f N^0 \ (1-\exp(-\lambda T))} \tag{3.6}$$

D (t) is the minimum detectable disintegration rate for the activation product corrected for the losses due to post-irradiation decay or assay [1].

3.1. GENERAL TECHNIQUE OF NAA

The selection of neutron activation analysis as the appropriate technique for the solution of an analytical problem is based on its sensitivity, speed, economy, convenience. In general these conditions have to be considered when solving a given analytical problem:

a) The selection of an appropriate nuclear reaction for activation analysis is based on the physical, chemical, and nuclear properties of the matrix and trace elements and of their activation products. These properties determine the sensitivity with which a given trace element can be measured, the importance of possible interfering reactions or competing activation products, the extent to which post-irradiation assay technique must be provided, and the practicability of providing a sample suitable for irradiation.

Generally, the principal technical considerations in the selection of suitable nuclear reactions are that they should

-produce radionuclides which are retained in the sample and have appropriate half-lives and decay characteristics for accurate measurements,

-have optimum or sufficient sensitivity,

-have no reactions producing competing radioactive isotopes of the same element as the activation product and that the requisite irradiation and post-irradation are feasible.

b) Theory and calculated sensitivity estimates. The Sensitivity depends according to Eq. (3.6), on the type of instrumentation used, nuclear factors, such as, interfering reactions or the macroscopic cross-section of the matrix. These factors limit the duration or intensity of irradiation or the size of the sample. The basic equation for the activity R generated by exposure to a thermal neutron flux ϕ for a period of time T is

$$R = \phi\sigma n(1 - \exp(\frac{-0.693T}{t_{1/2}})) \qquad (3.7)$$

where n is number of target nuclei, capable of forming the radioisotope in question by (n,γ) reaction, σ is the isotopic thermal neutron cross-section, and $t_{1/2}$ is the half-life of the isotope formed.

Eq. (3.7) show that the activity produced is directly proportional to the neutron flux, ϕ, hence the minimum detectable amount and concentration of an element are inversely proportional to the flux. Saturation activity(R_s) is achieved if T is very large compared to $t_{1/2}$, then the expression becomes

$$(1 - \exp(\frac{-0.693t_i}{t_{1/2}})) \Rightarrow 1$$

From rel. (3.7) one can also see that, if

$t_i = t_{1/2}$ then $R = \frac{1}{2} R_s$

$t_i = 2\ t_{1/2}$ then $R = \frac{3}{4} R_s$

$t_i = 3\ t_{1/2}$ then $R = \frac{7}{8} R_s$

We see that, if there is interest only in a short-lived activity, the sample need not be activated for more than one or two half-lives of the activity being produced. This is an important advantage of the instrumental method, because it permits the approach of saturation activity levels with short irradiation times, if we are dealing with rather short half-lives [13]

c) Choice of a suitable irradiation facility. The selection of an irradiation facility is based primarily on the type of nuclear particle required. The selection of a particular facility may also be based on the intensity required to achieve the desired sensitivity and the energy of the neutrons required

d) Preparation of samples for irradiation.

The physical, chemical and nuclear properties of the constituents of a sample and the

properties of their activation products dictate the pre-irradiation treatment of the sample. Nuclear considerations may limit the mass of the samples in neutron irradiation.

For neutron irradiation, the dimensions of the sample are normally limited by:

- the size of the available irradiation space
- the nuclear properties of the sample or its activation products
- the quantity of sample required to obtain the necessary sensitivity
- the quantity available for analysis .

The nuclear properties of the sample or its activation products are probably the most important. The limiting nuclear considerations may be the intensity of activation of the sample, which may present a radiation hazard in the laboratory, or a self-shielding within the sample due to its high cross-section.

e) Irradiation

Two general irradiation and analytical technique apply to neutron activation analysis. These are commonly referred to as the absolute assay technique and the comparative assay technique.

The absolute assay technique requires the activation be carried out in a neutron flux, that the pertinent nuclear date be known accurately and that the radiometric assay be quantitative. For the measurement of absolute disintegration rates of the activation product suitably calibrated instruments are required.

The comparative assay, or comparator technique utilizes standard samples of the trace elements which are irradiated simultaneously with the samples and assayed in the same manner. Good accuracy in the analysis of unknown element can be realized by a procedure involving comparative measurements with samples of known composition are subjected to an irradiation in an arrangment identical with that for the unknowns, and if possible at the same time [13]. Since this technique requires relative measurements only and eliminates the

need for certain accurate nuclear data, it usually yields more accurate analytical results with greater convenience than the absolute assay technique.

The optimum length and intensity of the irradiation are normally determined by the required sensitivity and the half-lives of the trace element activation products. However, the activation of the major constituents of the sample or the presence of reactions limit either the length or the intensity of the irradiation. The irradiation time is an essential parameter for the simplification of the γ–ray spectrum produced by a complex sample. Thus, a brief irradiation, followed by rapid counting, produces a spectrum in which the short-lived activities developed in the sample are accentuated. Similarly, a longer irradiation, followed by an appropriately long decay time before counting, produces a spectrum in which the longer lived activities developed in the sample predominate [12].

In activation analysis with sources of low flux the statistical error occurring of the randomness of radioactive decay is one of the principal errors. The probable error in a counting determination giving 'C' counts is $0.67\sqrt{C}$. Hence the more counts that can be obtained for a given sample the more certain the determination of sample activity [14].

3.2. TYPES OF NEUTRON ACTIVATION ANALYSIS

Different sources are used for the bombardment of the sample by neutrons. Most of the work has been done with thermal neutrons from reactors and some with fast neutrons from neutron generators.

3.2.1. NEUTRON ACTIVATION ANALYSIS WITH THERMAL NEUTRONS

The neutrons produced by radioisotope neutron source are slowed down by elastic collisions with moderator atoms until equilibrium is reached with thermal motion of the moderator atoms. Thermal neutrons interact with nuclei predominantly through the (n,γ) reactions. All stable isotopes are capable of capturing thermal neutrons, but have characteristic capture cross-sections that vary widely from nucleus to nucleus. If the product nucleus is radioactive, its later decay can be detected and used for activation analysis [15]. The resulting nucleus de-excites by emission of γ-rays.

Thermal neutrons are mostly used for neutron activation analysis, because of large cross-sections of many elements. For neutron activation analysis with thermal neutrons, we are going to use one of the two detector types:

-NaI (Tl) detector,

-Ge detector.

Neutron activation analysis by thermal neutrons is used mainly for concentration measurements of different elements in the sample.

3.2.2. FAST NEUTRON ACTIVATION ANALYSIS

Fast neutrons interact with nuclei predominantly by (n,α), (n,p), $(n,2n)$ and (n,n') reactions. Fast neutron activation analysis is mostly carried out by 14 MeV neutrons

because of the availability of neutron sources. Activation analysis with 14 MeV neutrons is applied mainly to the determination of light elements because it has the advantage of high sensitivity for light nuclei [15].

4. EXPERIMENT

The study was performed using neutrons from an Am-Be neutron source. Copper, brass as well as Ni, I and Mn (in chemical compounds) were used to show the capabilities of NAA. In case of the ^{63}Cu (n,γ) ^{64}Cu reaction the electronic arrangement was designed to detect the 511 keV annihilation photopeak of copper-64. Further details of the experiment are given below.

4.1 EXPERIMENTAL SET UP

The basic parts of the experimental set up are the detector, the electronics plus the data storage system and the neutron source. Fig. 4.1 shows a block diagram of the experimental set up for γ–ray measurements.

4.1.1 THE COAXIAL GERMANIUM DETECTOR

The coaxial germanium detector is basically a cylinder of germanium with an n-type contact on the outer surface, and a p-type contact on the surface of an axial well. The germanium has a net impurity level of around 10^{10} atoms/cm^3 so that with moderate reverse bias, the entire volume between the electrodes is depleted, and an electric field extends across this active region. Photon interaction with this region produces charge carriers which swept by the electric field to their collecting electrodes where a charge sensitive amplifier converts this charge into a voltage pulse proportional to the energy deposited in the detector. The specification and performance data of the detector used is given in appendix A.

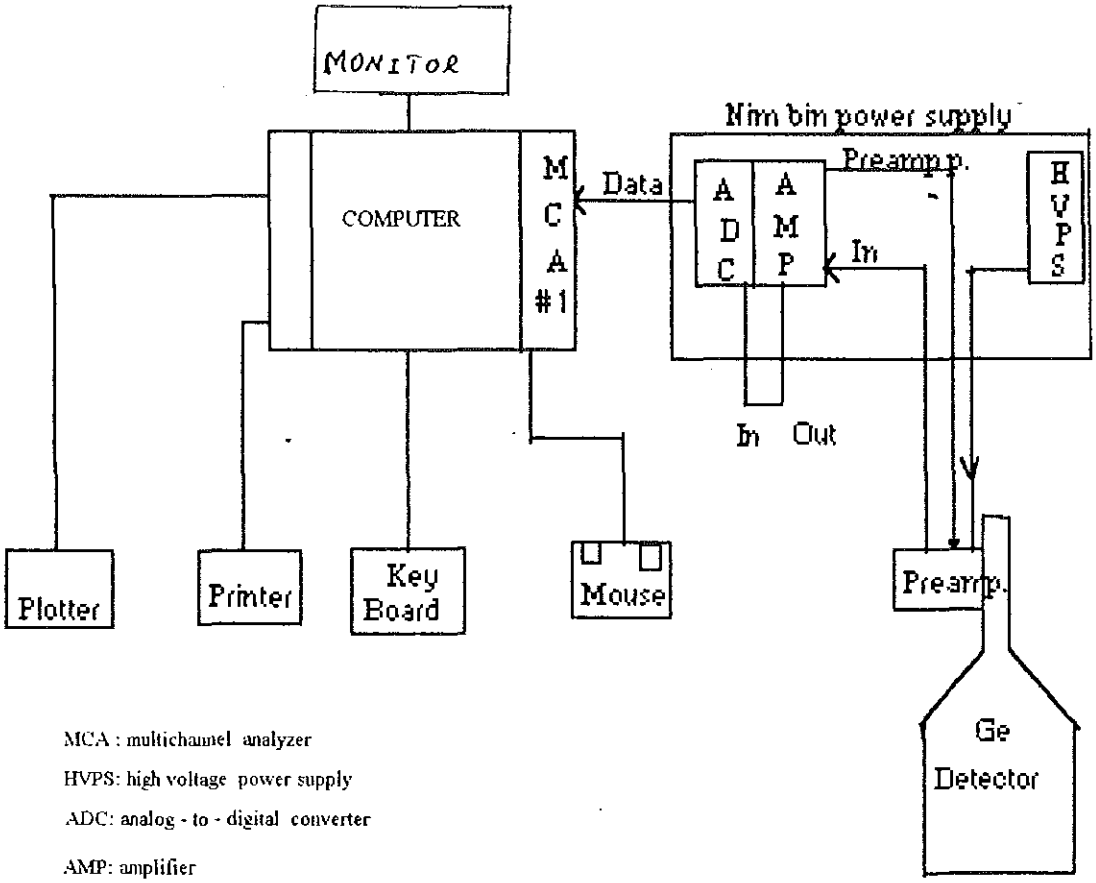

Fig.4.1. Experimental set up for measuring gamma-ray spectra

4.1.2 ELECTRONICS

The electronics of the spectrometer consists of a detector bias supply, preamplifier, amplifier, analog- to- digital converter, data storage device and computer. In this electronic system, which is shown in Fig. 4.2 , the pulses from the Ge detector was amplified, fed to a linear amplifier, and through an analog- to - digital-converter to MCA and PC.

a. DETECTOR HV POWER SUPPLY

The HV module is basically a dc-to-dc converter. The input to the high voltage dc-to-dc converter is obtained from a conventional Nim power supply and uses +- 12 V and +-24 V.

The HV amplification is a function of a control voltage in which the sensing circuit generates the control voltage to set and maintain a fixed high voltage [16]. In order to collect the charge formed in the detector, a bias voltage was placed across the detector. Its operating voltage depends on the size of the detector.The optimum bias voltage of the detector used is 3500V. The voltage which is applied to the detector ought not to be subjected to rapid change.

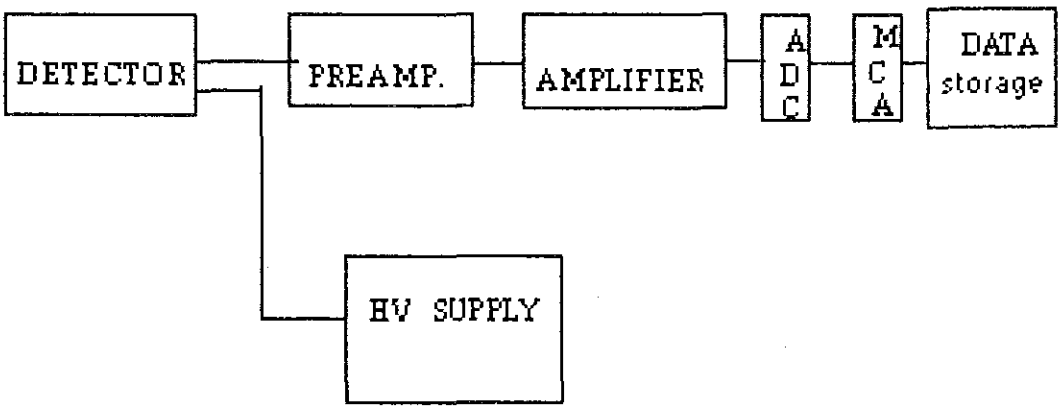

Fig. 4.2 Schematic diagram of the electronic system

b. PREAMPLIFIER

In order to minimise the electronic noise, the input stage of the preamplifier, usually a field-effect transistor stage, is cooled in the same manner as the detector. The preamplifier includes a feed back circuit. The amplitude of the pulse from the preamplifier should be proportional to the amount of charge collected in the detector.

c. AMPLIFIER

The model 2024 spectroscopy amplifier with its selection of shaping time constants was used. The choice of shaping time allows the best possible performance by tailoring the system for the conflicting requirement of optimum signal to noise ratio and high count rate performance.

The model 2024 amplifier was shipped with the restorer response jumper plug in the linear response position, which will give the best restorer response for shaping time constants. Additionally, there is a jumper plug to invert the logic sense of the pileup rejector incoming inhibit signal and another for the output reject signal. The model 2024 was inserted into a standard NIM bin. Preamplifier power was provided by means of a connector located on the rear panel of the model 2024 amplifier. The model 2024 amplifier controls were set as indicated below

Shaping time..... 2μs

Coarse gain..... 100

Fine gain.....7.2

Restorer mode..... ASYM

Restorer threshold..... AUTO

The input polarity switch was set to match the output polarity of the preamplifier (positive) In order to exploit fully the count rates capabilities of the model 2024 amplifier, the ADC was direct coupled for linear-input signals.

d. ANALOG - TO - DIGITAL CONVERTER AND DATA STORAGE

The Canberra model 8075 is a single-width Nim analog - to - digital converter for application in nuclear spectroscopy. The basic task in gamma spectrometry is the measurement of the pulse-height distribution at the amplifier output. The analog - to - digital converter (ADC) converts the analog output information of the amplifier into a digital quantity. The pulse height information from ADC stored in array which gives the cumulative number counts observed in each channel [17]. The information of the pulse height was acquired using a special software (S-100 system). This programme package allows to accept the ADC output signals, controls the counting duration, displays the data as it is taken, do simple data processing and transfer the data on request to another device.

The electronic system also determines the effective duration of the measurement. The dead time is indicated for each data taking.

4.1.3 NEUTRON SOURCE

A 2 Ci Am-Be neutron source was used. In the ^{241}Am-Be source, the amercium-241 alloyed with beryllium, the alpha particles from americium have sufficent energy to react with beryllium which causes emission of neutrons according to the reactions

$$^{241}\text{Am} \rightarrow \quad ^{237}\text{Np} + {}^{4}_{2}\text{He}$$

$$^{4}_{2}\text{He} + {}^{9}_{4}\text{Be} \rightarrow \quad {}^{12}_{6}\text{C} + {}^{1}_{0}\text{n}$$

The neutron yield of the source is approximately 77 neutrons per 10^6 alpha particles with an average energy of 4.5 MeV[18]. The energy distribution from an ^{241}Am-Be source is given in Fig. 4.3 .

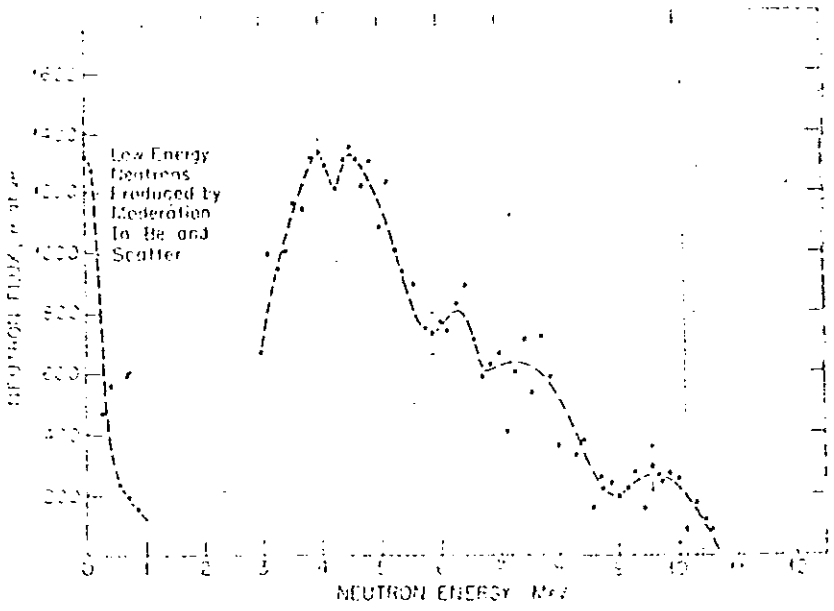

Fig. 4.3 Neutron energy distribution from an ^{241}Am-Be neutron source [18]

The ^{241}Am-Be source is surrounded with a paraffin wax as a moderator to thermalize the neutrons and insulated in the centre of the assembly as shown in Fig.4.4. The holder fitted over the irradiation channels during irradiation (the main characteristics of the neutron

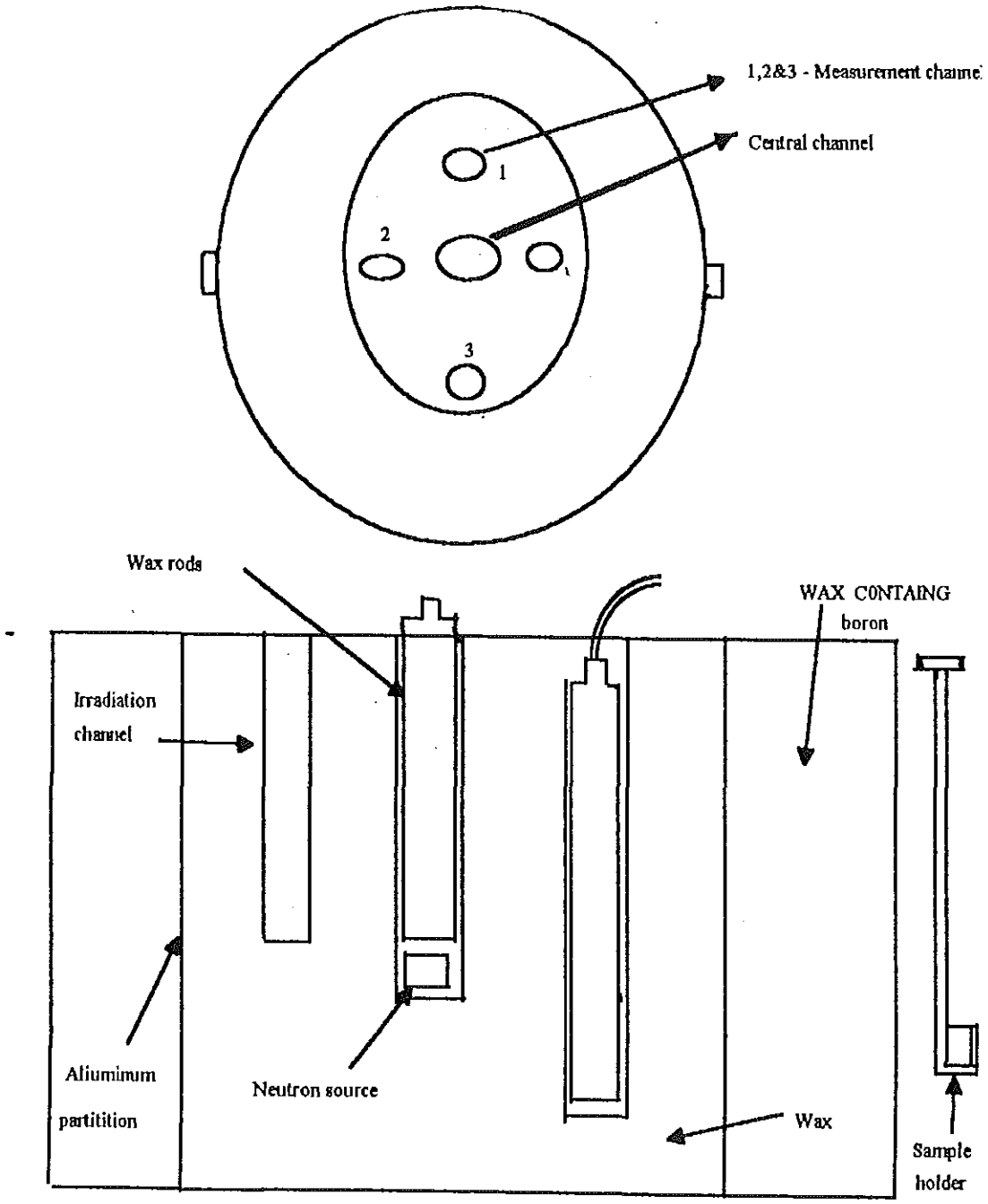

Fig. 4.4 Schematic diagram of ^{241}Am-Be neutron source

4.2. EXPERIMENTAL PROCEDURE

After measuring the sample mass by a balance, the sample was introduced into the sample holder for NAA. The sample was inserted direct into the irradiator, and the timing of irradiation was recorded. At the end of the pre-set irradiation time, the sample was removed from the irradiator and transferred manually to the detector, and the actual duration of the irradiation was recorded . The counts were recorded mostly for 1000 seconds.

5. DATA ACQUISITION

Before the measurement of activation spectra a background spectrum should be measured for a longer time. An example of the background spectrum is shown in Fig. 5.1.

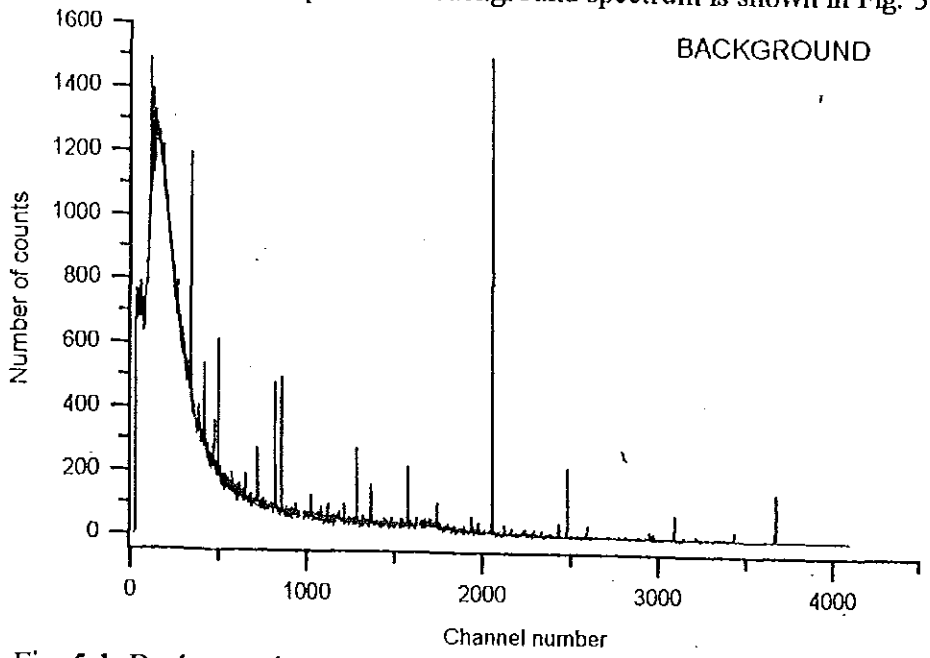

Fig. 5.1 Background spectrum measured for 1000s of the experimental room without using a passive shielding

5.1. LIFE TIME MEASUREMENTS

By repeated scans of the gamma spectra of the samples at various intervals of time, the decay of the isotope is obtained from the decrease in the area of the respective photopeaks. The value of the half-life of the isotope obtained in this manner can then be used to confirm the presence of a single radionuclide[19]. Because of this extensive measurements were carried out to collect information on the life-time of activated copper-64 using the Cu^{63}(n,γ) Cu^{64} reaction. The γ–spectrum contains the characterstics 511 keV annihilatioon line according to the decay scheme shown in a Fig. 5.2 All.data were collected with the Canberra S-100 data acquisition system. The corresponding measurements for copper and brass samples are given in tables 5.1, 5.2, and 5.3.

Examples of γ–spectra measured with copper and brass samples are shown in figs. 5.3, 5.4, and 5.5

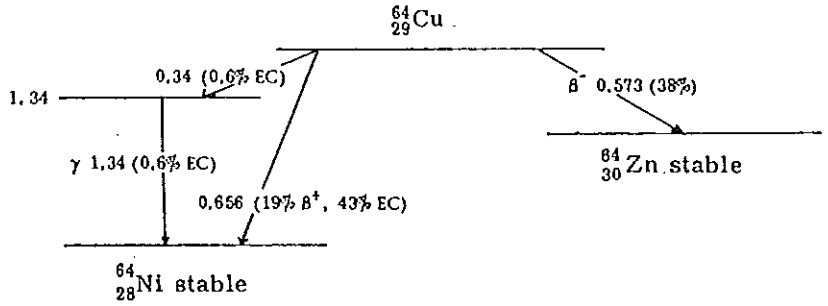

Fig. 5.2 Schematic diagram of ^{64}Cu

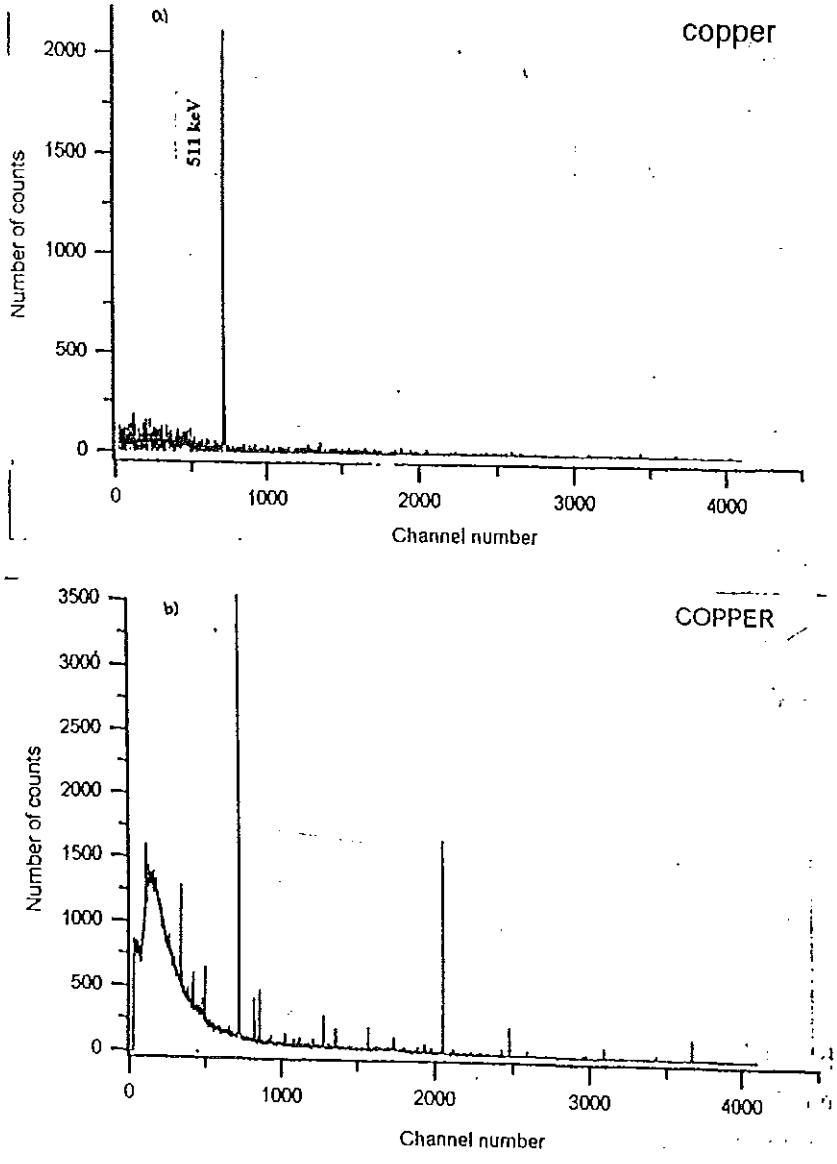

Fig. 5.3 Gamma ray spectra observed with Ge detector of pure copper sample irradiated in ^{241}Am-Be neutron source for 24 h a) without background b) with background

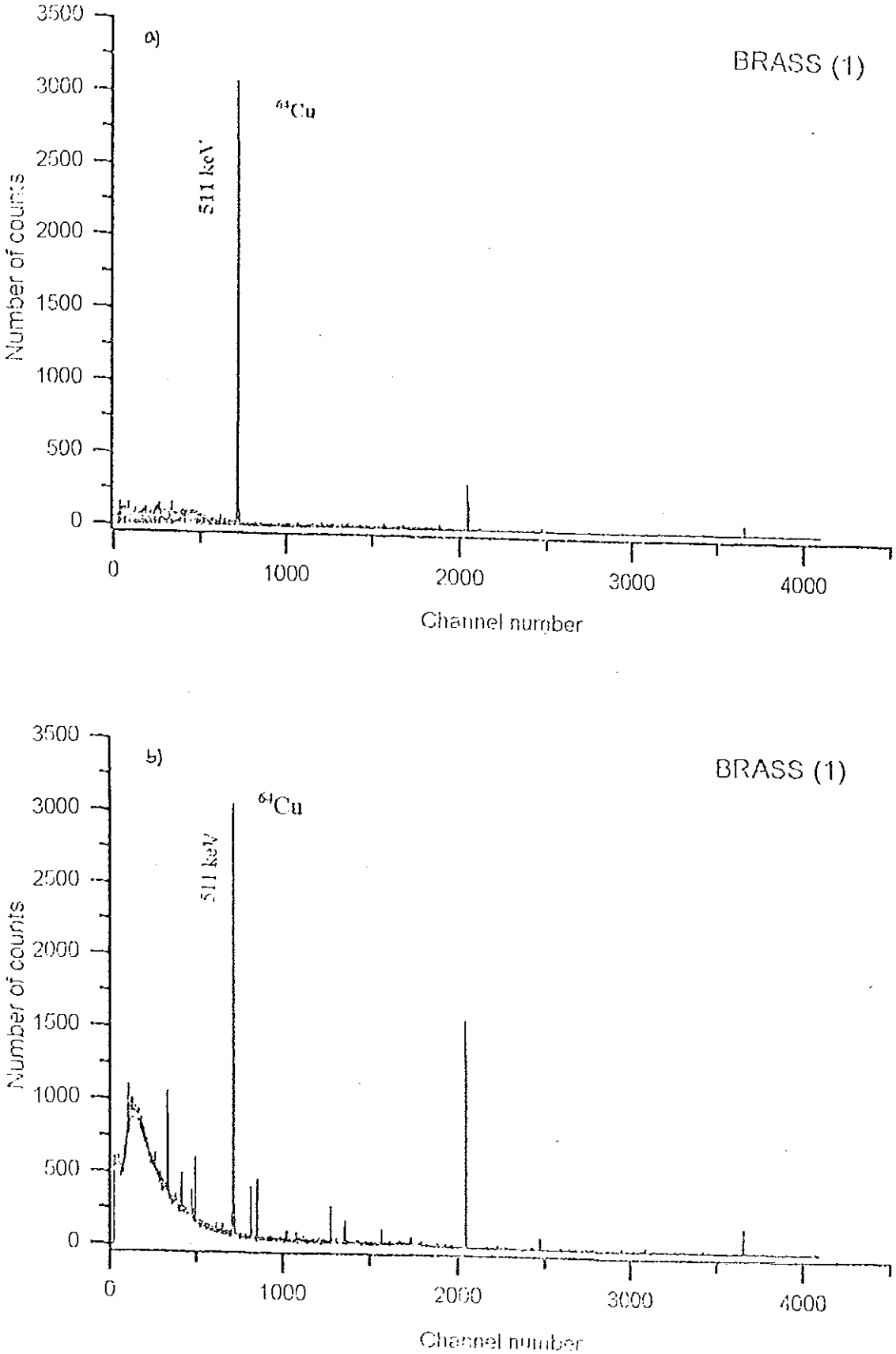

Fig. 5.4 Gamma -rays spectra observed with Ge detectoAr from brass sample number one irradiated by an ^{241}Am-Be neutron source for 24 h a) without background b) with baelground

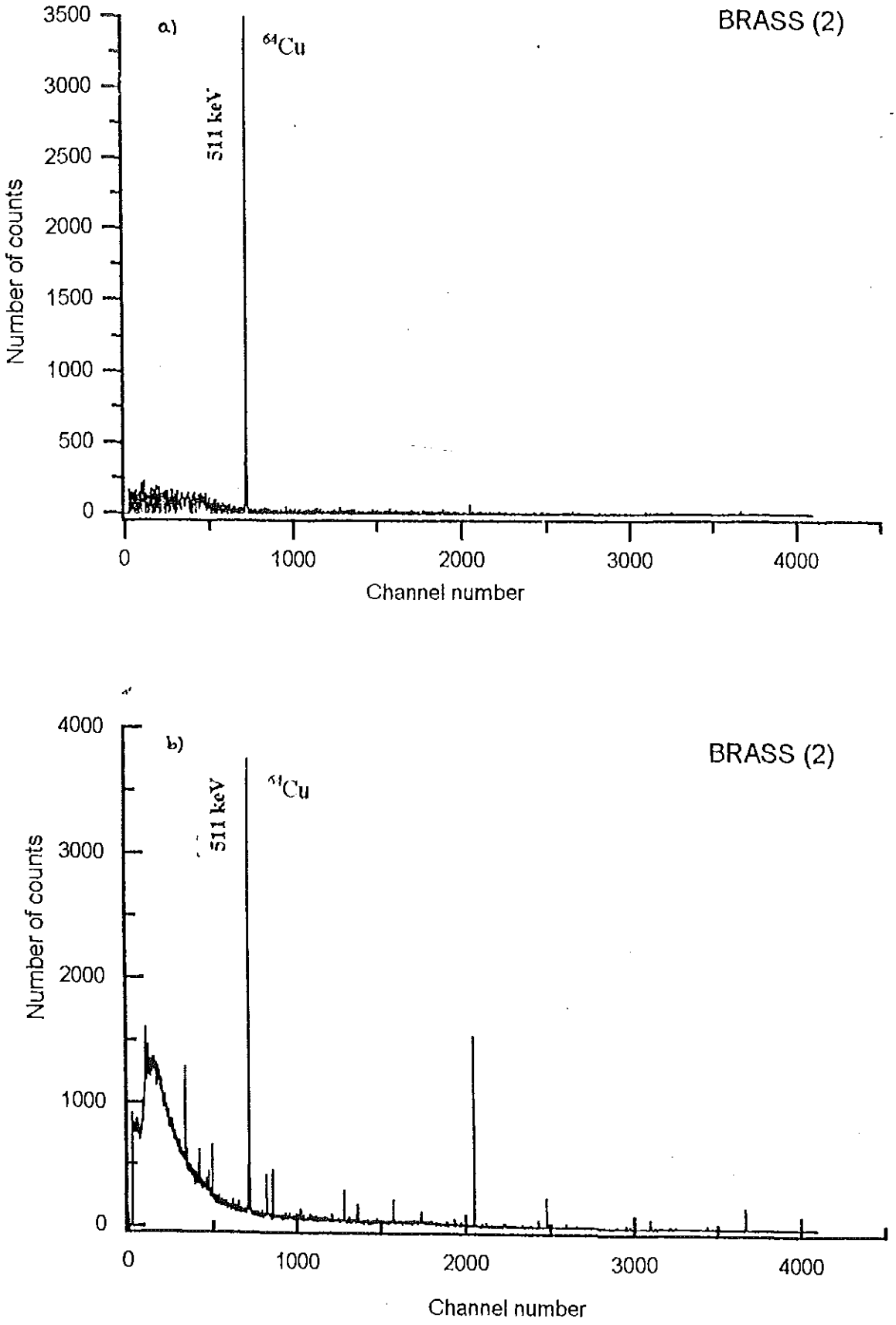

Fig 5.5 Gamma-ray spectra observed with Ge detector from brass sample number two irradiated by an ^{241}Am-Be neutron source for 96 h a) without background b) with background

Table 5.1 Decay data for pure copper (1)[1]

Data without Background	
Time After Irradiation (h)	Area of the line (counts)
2.26	13737 +/-1.5%
3.38	13008+1.6%
4.29	12048+/-1.7%
5.37	11663+/-1.7%
6.42	11004+/-1.7%
7.46	10556+/-1.7%
8.56	9714+/-1.8%
9.59	9480+/-1.8%
10.63	8690+/-1.9%
11.63	8348+/-2.0%
23.50	4457+/-2.5%
22.43	4473+/-2.7%
24.55	4041+/-2.8%
25.60	3892+/-2.9%
26.56	3672+/-2.9%
27.65	3500+/-3.0%

[1] Copper(1) is the standard copper sample which is irradiated by an ^{241}Am-Be neutron source for 96 h.

Table 5.2 Decay data of Brass (2) sample [1]

Data withoutbackgrond	
Time after irradiation (h)	Area of the line (counts)
0.6	14435+/-1.5%
2.93	12970+/-1.6%
3.64	12424+/-1.6%
4.66	11957+/-1.7%
5.54	11295+/-1.7%
6.61	10285+/-1.8%
7.69	9949+/-1.8%
8.74	9313+/-1.8%
9.76	8774+/-1.9%
10.79	8429+/-1.9%
11.77	7825+/-2.0%
22.78	4334+/-2.7%
23.83	4213+/-2.7%
24.00	3827+/-2.9%
	3709+/-2.9%
26.95	3578+/-3.0%
27.95	3263+/-3.2%

[1] Brass is the second brass sample which is irradiated by ^{241}Am-Be neutron source for 96 h.

Table 5.3 Decay data for Brass (1) [1]

Data without background	
Time after irradiation(h)	Area of the line
1.33	12092+/-1.6%
2.42	11556+/-1.7%
3.52	10697+/-1.7%
4.62	10188+/-1.8%
5.85	9701+/-1.8%
6.85	9232+/-1.9%
7.92	8544+/-1.9%
9.00	7954+/-2.0%
10.1	7730+/-2.0%
11.18	7041+/-2.2%
12.25	6748+/-2.2%
23.62	3636+/-2.2%
26.87	3226+/-2.3%
27.50	3088+/-2.4%

[1] Brass (1) is brass sample number one which is irradiated by an ^{241}Am-Be neutron source for 24 h.

5.2 CONCENTRATION MEASUREMENT OF ^{64}Cu IN BRASS

In Fig. 5.6, 5.7, and Fig. 5.8 spectra are shown in which the peaks are labelled by their photopeak energies.

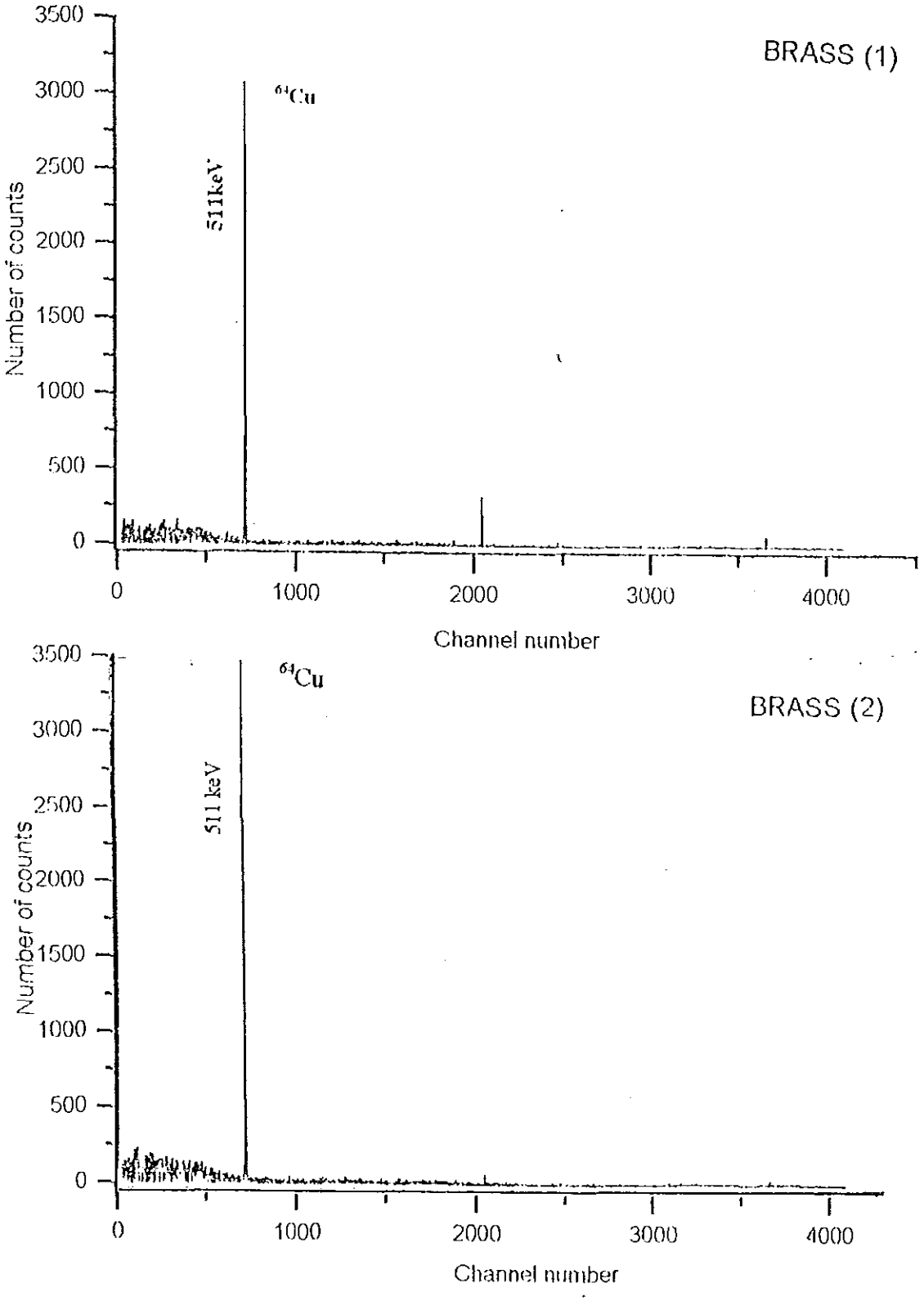

Fig. 5.6 Gamma-ray spectra observed with Ge detector from the activation of brass with with thermal neutrons from ^{241}Am-Be neutron source.

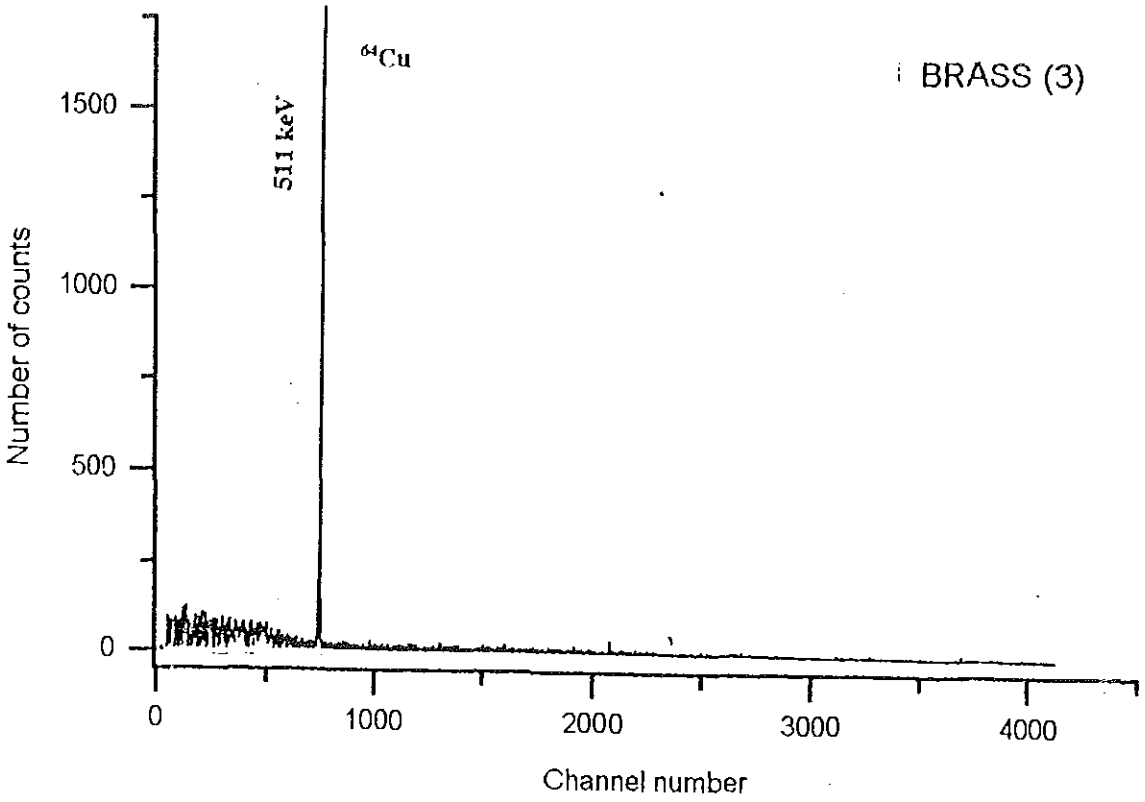

Fig. 5.7 Counts versus channel number of gamma-ray spectra observed with Ge detector from activation of brass with thermal neutrons from ^{241}Am-Be neutron source.

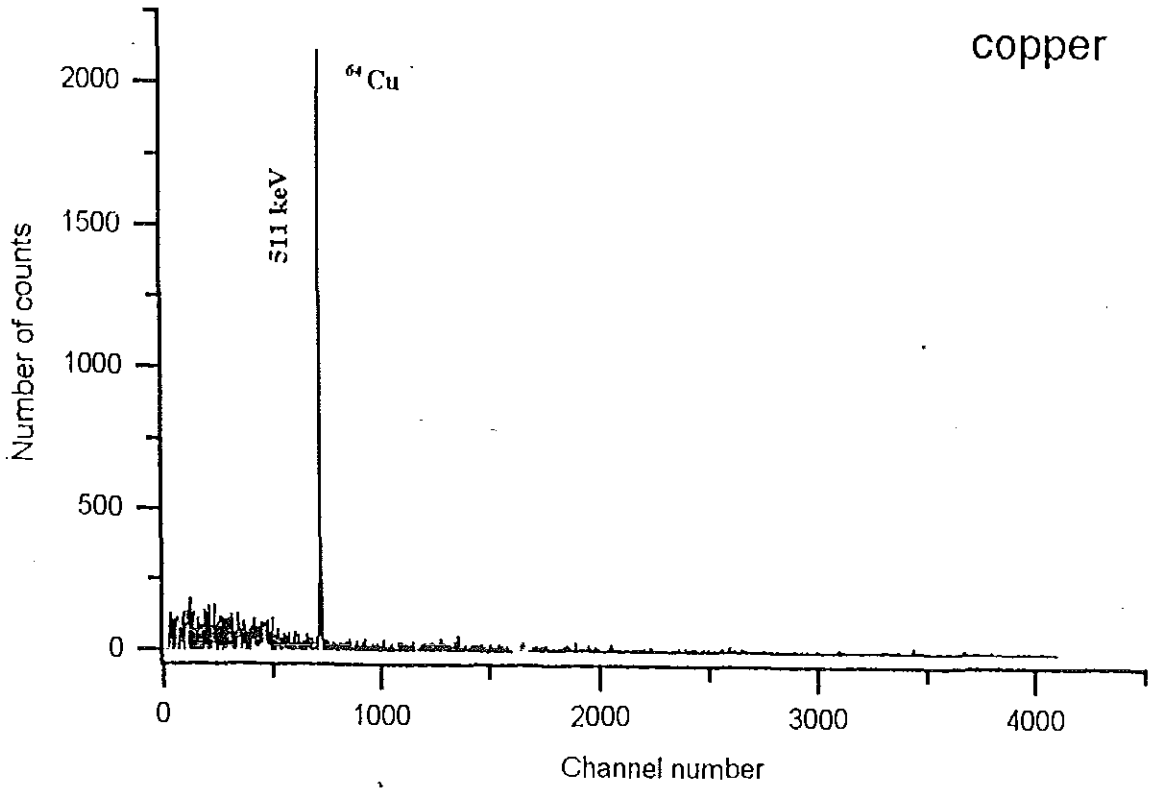

Fig. 5.8 Gamma-ray spectra observed with Ge detector from activation of copper with thermal neutrons from ^{241}Am-Be neutron source

The gamma ray at 511 keV are seen in all spectra. The amount of copper-64 in the sample were determined due to its 511 keV peak in the gamma ray spectra. The 511 keV peak area and the corresponding mass of brass samples are listed in table 5.5.

Table 5.5 Area of the photopeak line and the mass of the samples

Sample	Peak area at 511 keV (counts)	Mass(g)	Plate thicknèss(m.m)	Measuring time after irradiation(hr.)
copper	13945+1.59%	2.35	4.00	1.41
brass(1)	12501+1.68%	3.35.	4.00	1.33
brass(2)	15027+1.52%	3.55	4.oo	1.26
brass(3)	6440+2.40%	1.5	4.00	1.34
brass(4)	7400+2.01%	3.67	2.50	1.56

5.3. ADDITIONAL EXPERIMENTS IN NAA

We have measured spectra containg signals from I, Mn and Ni in order to show that NAA works for other elements using ^{241}Am-Be neutron source . The specra are given in Figs. 5.9, 5.10 and 5.11

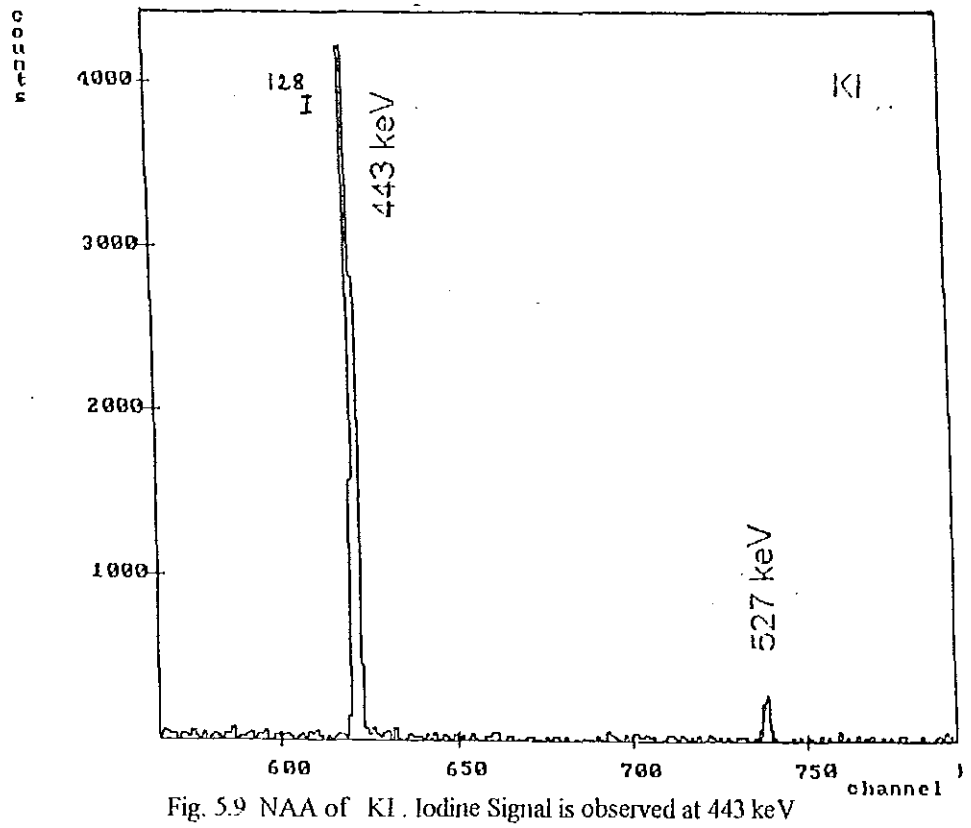

Fig. 5.9 NAA of KI . Iodine Signal is observed at 443 keV

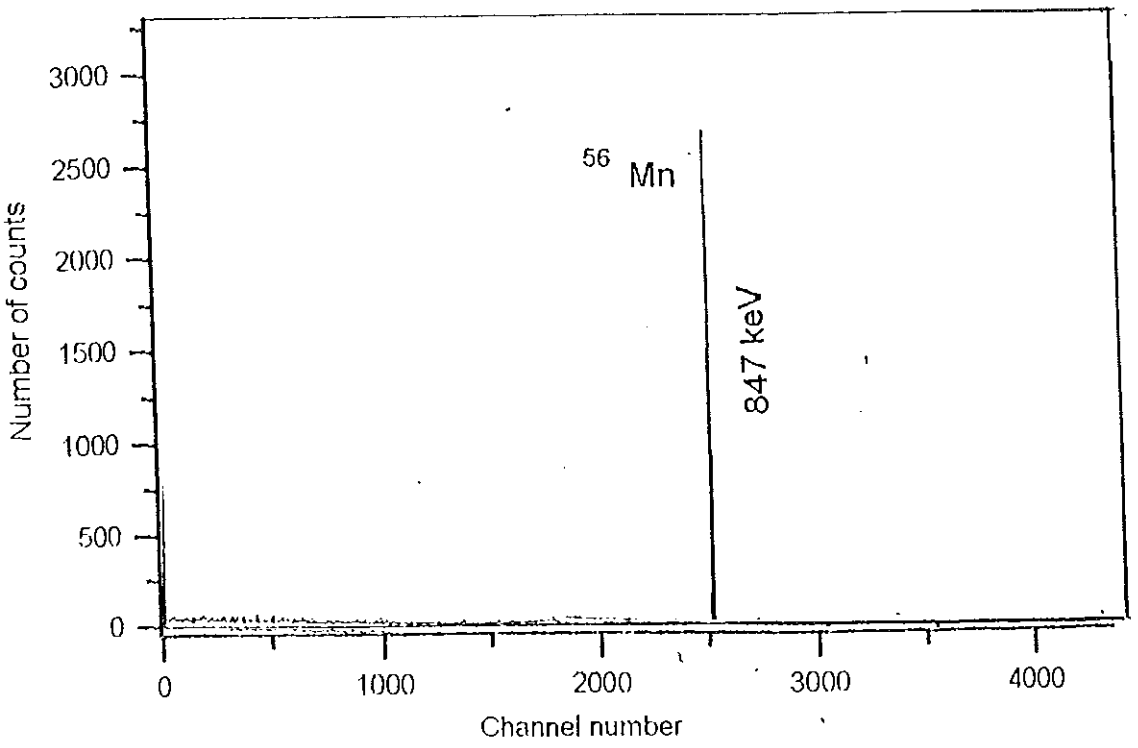

Fig. 5.10 NAA of $KMnO_4$. At 847 keV there appears the signal from Mn.

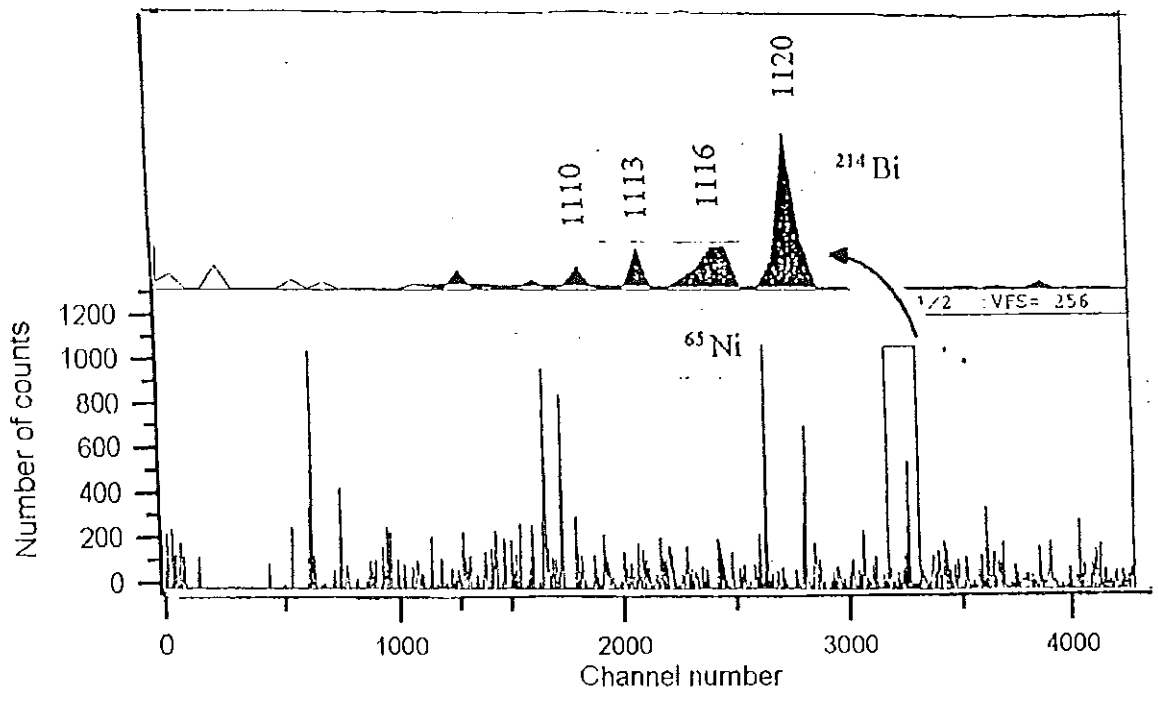

Fig. 5.11 NAA of a nickel sample. Nickel signal is observed at 1116 keV

6. DATA ANALYSIS AND DISCUSSION

In all the experiments performed the Ge detector was unshielded. The background radiation from the atmosphere, building materials and cosmic radiation was measured, examples are given in Fig. 5.1 and 6.1. The main radioactive nuclides responsible for the background were identified according to their energy. These identified radionuclides are shown in Fig. 6.1(b). After identifying the elements which are responsible for the background spectrum, the half-life of copper-64 isotope was determined. The measured data for copper and brass samples are given in table 6.1, 6.2 and 6.3, respectively. From the measured data and spectra of the standard copper sample, it is clear that the 511 keV annihilation line was similar with those found in brass samples due to its copper content. The half-life determined for the annihilation line of the copper sample is also similar to that of the exact value in literature.

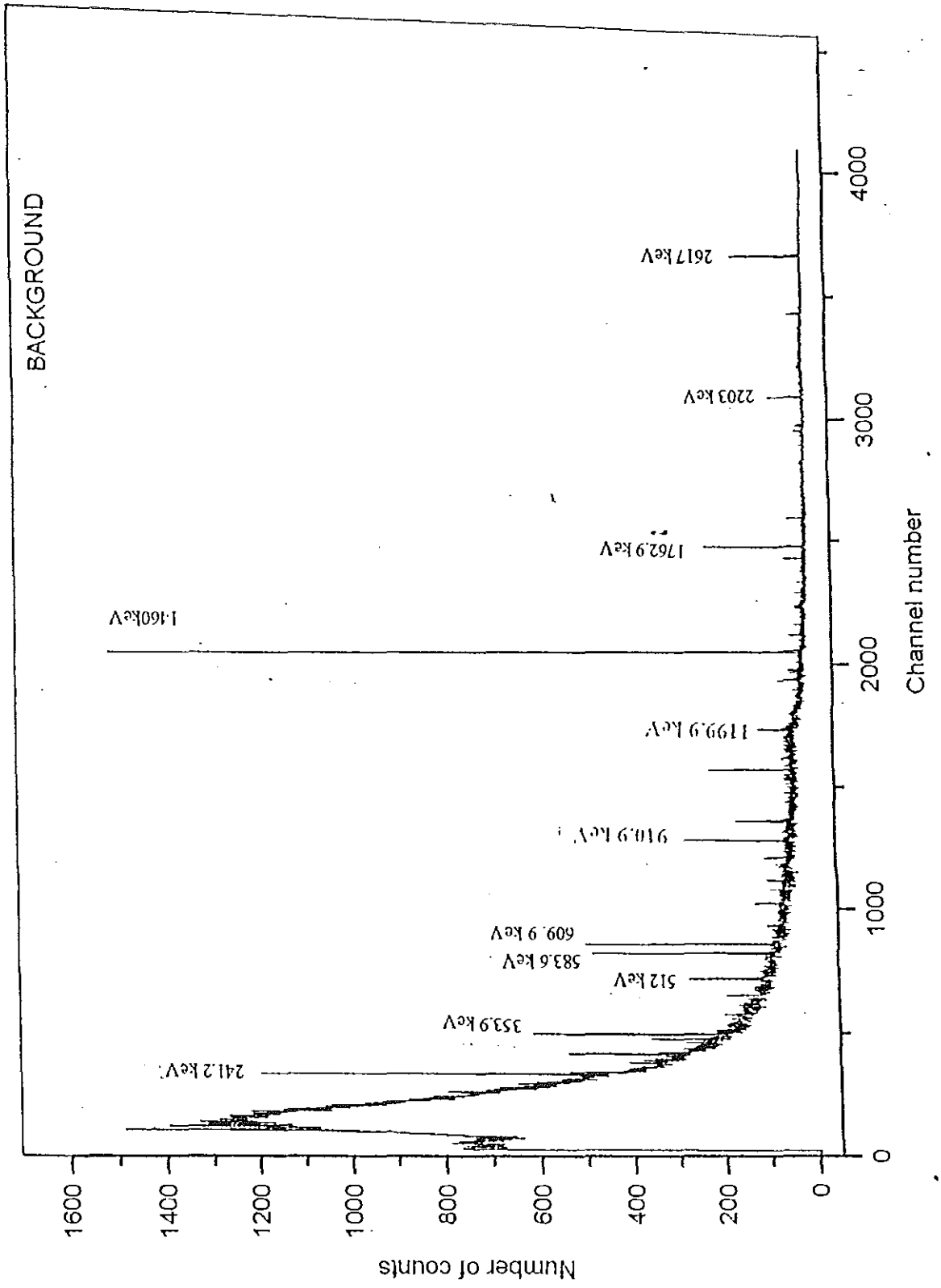

Fig. 6.1 (a) Ilustration of the background spectrum in enlarged form

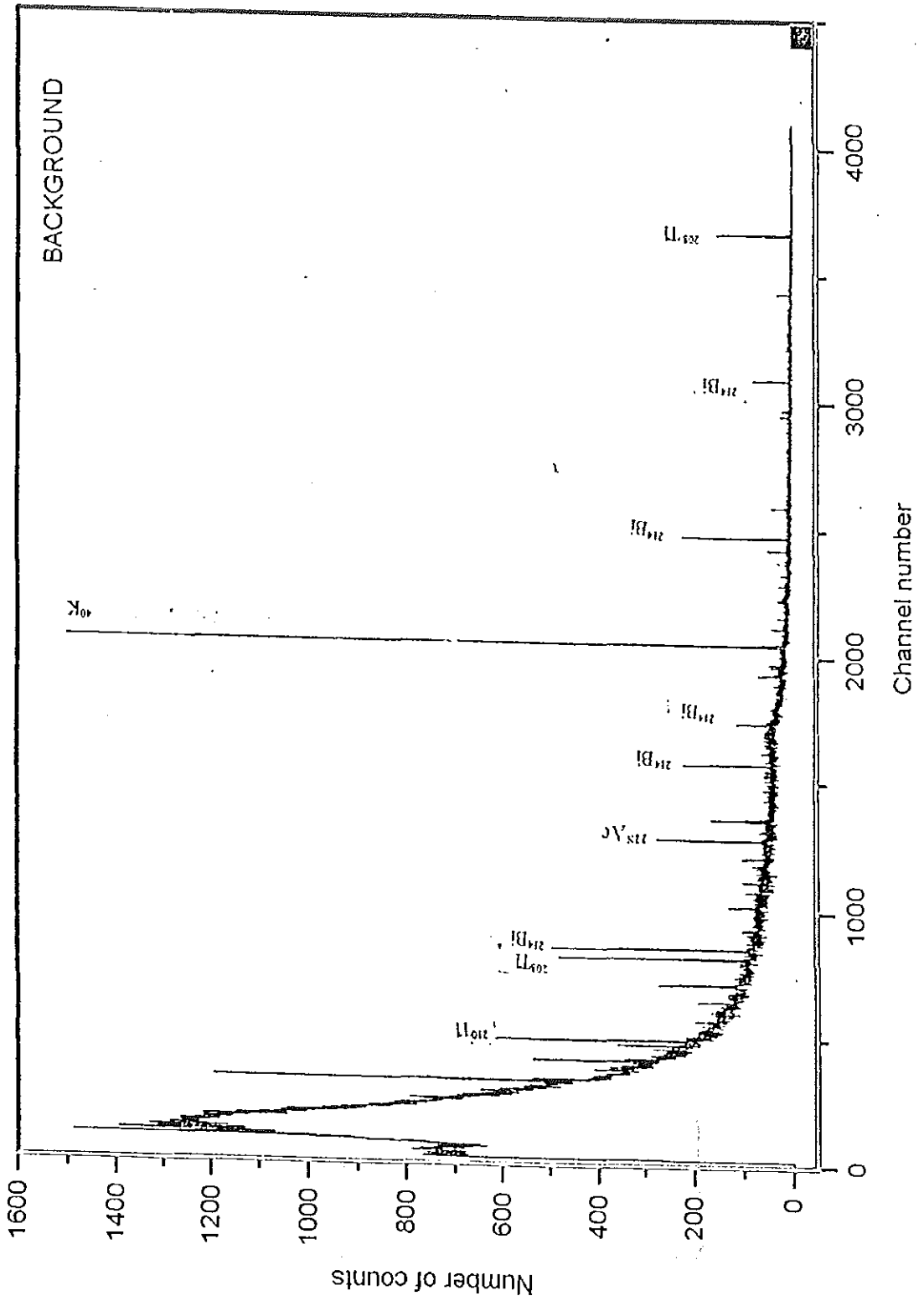

Fig. 6.1 (b) Illustration of the background spectrum in expanded form

Table 6.1 Evaluated decay data for pure copper

Evaluated decay data without background			
Time(h)	Area (counts/sec.)	Probable error[1] (+/-)	ln N +- σ/N [2]
2.26	13.737	1.56	9.5278+-0.008
3.38	13.008	1.46	9.4733+-0.009
4.29	12.048	1.303	9.3967 +- 0.00911
5.37	11.663	1.235	9.3642 +- 0.00925
6.42	11.004	1.11	9.3060 +- 0.00953
7.46	10.556	1.014	9.2644+- 0.00973
8.56	9.714	0.81	9.1569+- 0.01015
9.59	9.480	0.74	9.1569+- 0.01002
10.63	8.690	0.44	9.0699 +- 0.01072
11.63	8.348	0.19	9.0298 +- 0.01094
22.43	4.457	1.31	8.4022+- 0.01497
23.5	4.473	1.31	8.4058 +- 0.01495
24.55	4.041	1.38	8.3042+- 0.01573
25.6	3.892	1.40	8.2667+- 0.01602
26.56	3.672	1.44	8.2085+- 0.01650
27.65	3.500	1.46	8.1605+- 0.01690

[1] Probable error = $0.67\sqrt{C}$, where C is the number of counts under the photpeak area.

[2] σ is the standard deviation of the count.

Table 6.2. Evaluated spectrum data for Brass (1).

Evaluated data without background			
Time (h)	Area (counts/sec.)	Probable error[1](+/-)	ln N +- σ/N^2
1.33	12.092	1.38	9.4003 +- 0.00969
2.42	11.556	1.289	9.3550 +- 0.00930
3.52	10.697	1.129	9.2777 +- 0.00967
4.62	10.188	1.023	9.2290 +- 0.00991
5.85	9.701	0.910	9.1800 +- 0.01015
6.85	9.204		9.1274 +- 0.01042
7.92	8.544	0.556	9.0530 +- 0.01082
10.1	7.730	0.236	8.9529 +-0.01137
11.18	7.041	0.604	8.8595 +- 0.01192
12.25	6.748	0.704	8.8170 +- 0.01217
23.62	3.636	1.376	8.1986 +- 0.01658
26.87	3.088	1.462	8.0353 +- 0.01760
24.7	3.226	1.441	8.0790 +- 0.01799

[1] Probable error = 0.67, where C is the number of counts under the photpeak area.

[2] σ is the standard deviation of the count.

Table 6.3 Evaluated decay data for brass (2).

Evaluated decay data without background			
Time(h)	Area (counts/sec.)	Probable error[1](+/-)	ln N +- σ/N^2
0.6	14.435	1.668	9.5774 +- 0.00832
2.93	12.970	1.457	9.4704 +- 0.00878
3.64	12.256	1.343	9.4138 +- 0.00903
4.66	11.788	1.262	9.3748 +- 0.00921
5.54	11.127	1.138	9.3171 +- 0.00948
6.61	10.285	0.958	9.2384 +-0.00986
7.69	9.949	0.876	9.2052 +- 0.01002
8.74	9.313	0.694	9.1392 +- 0.01036
9.76	8.774	0.489	9.0795 +- 0.01067
10.79	8.429	0.291	9.0394 +- 0.01089
11.77	7.825	0.432	8.9651 +- 0.01130
22.78	4.334	1.324	8.3742 +- 0.01518
23.83	4.213	1.345	8.3459 +- 0.0154
24.	3.827	1.407	8.2498 +-0.01616
25.93	3.709	1.426	8.2185 +- 0.01642
26.95	3.578	1.447	8.1826 +- 0.01671
27.95	3.263	1.495	8.0904 +- 0.0175

[1] Probable error = 0.67, where C is the number of counts under the photpeak area.

[2] σ is the standard deviation of the count.

From the data given in the tables 6.1, 6.2 and 6.3 the decay curve of copper-64 is plotted in Figs. 6.4, 6.5 and 6.6, respectively. The experimental decay constant for the ^{64}Cu was determined as the slope of the decay curve from the parameters of the linear fitting.

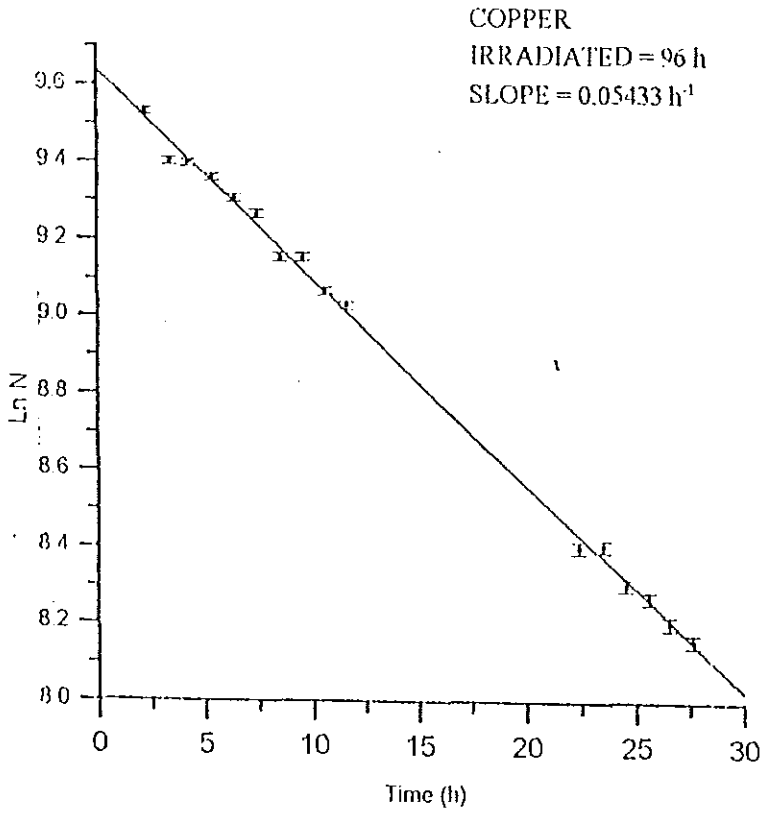

Fig. 6.4 Decay curve measured with the copper sample

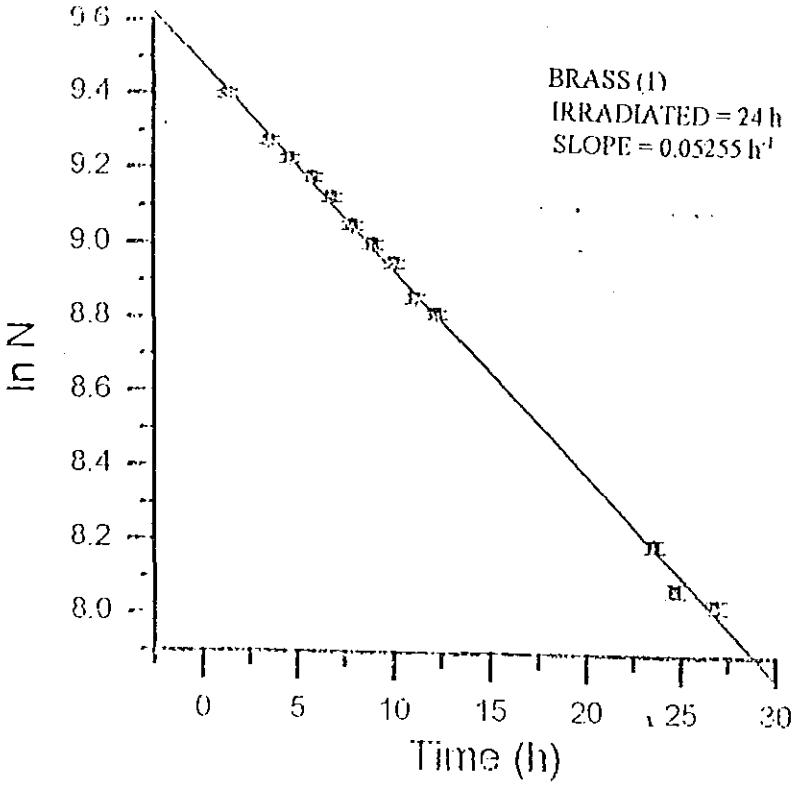

Fig. 6.5 Decay curve of brass (1)

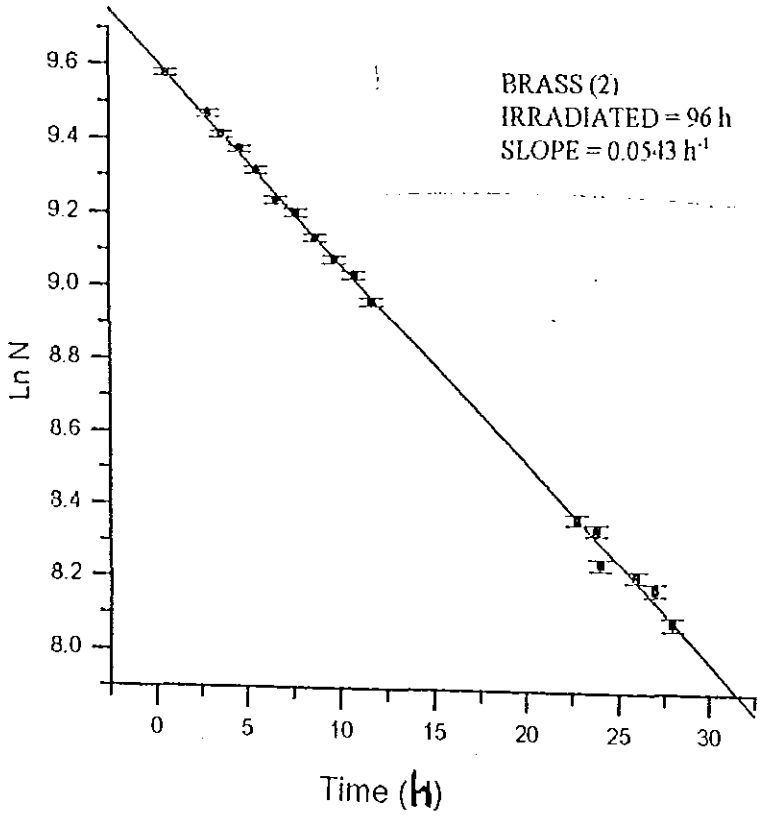

Fig. 6.6 Decay curve of brass (2)

Radioactive nuclides decay according to the exponential law

$$A = A_0 e^{-\lambda t} \qquad (6.1)$$

$$\ln A = \ln A_0 - \lambda t \qquad (6.2)$$

where A represents the measured activity at time t,

A_0 is the corresponding activity at $t = 0$, and λ is the decay constant related to the half-life

$$t_{\frac{1}{2}} = \frac{0.693}{\lambda} \qquad (6.3)$$

Rel. (6.3) is used to obtain the half-life for ^{64}Cu using the 511 keV photopeak of the activated brass sample.

In the first part of the experiment not only the half-life of copper-64 is determined. It is also shown that the decay curve of copper-64 follows an exponential decay curve, which is shown in Figs. 6.7, 6.8 and 6.9.

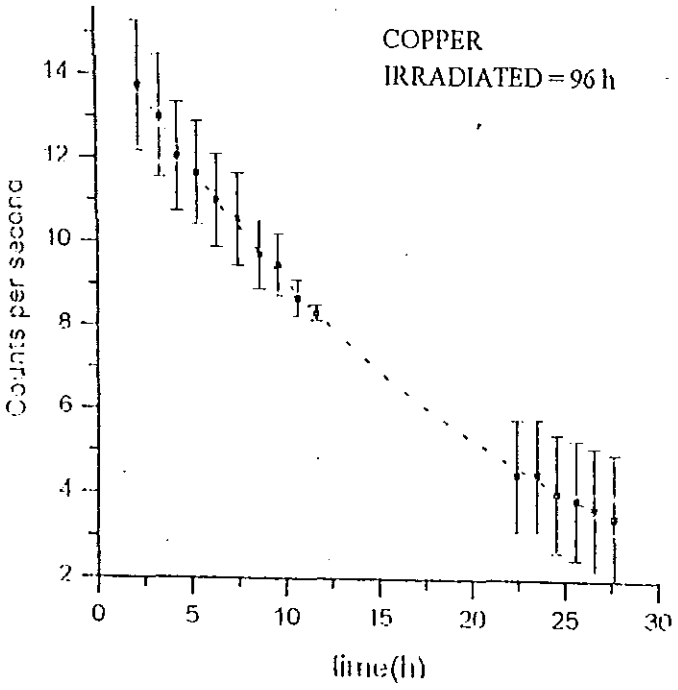

Fig. 6.7 Exponential decay of ^{64}Cu radionuclide in copper sample

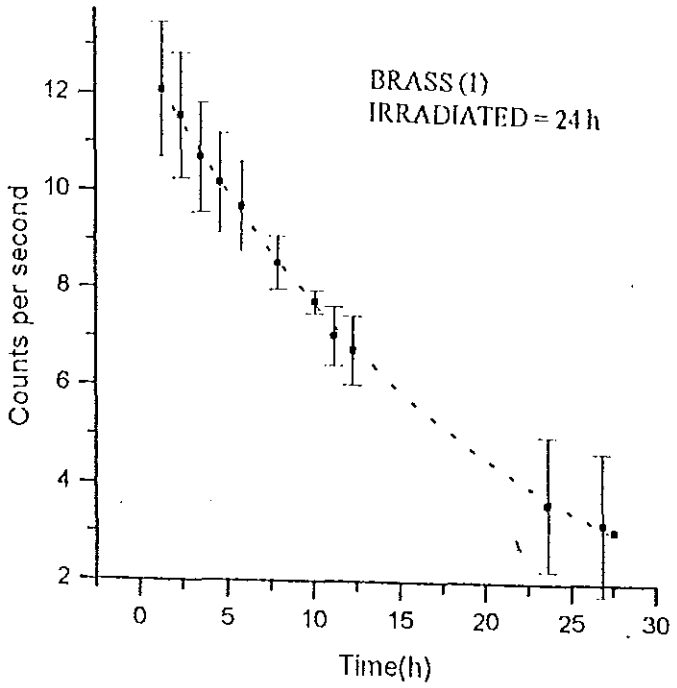

Fig. 6.8 Exponential decay of ^{64}Cu radionuclide in brass(1) sample

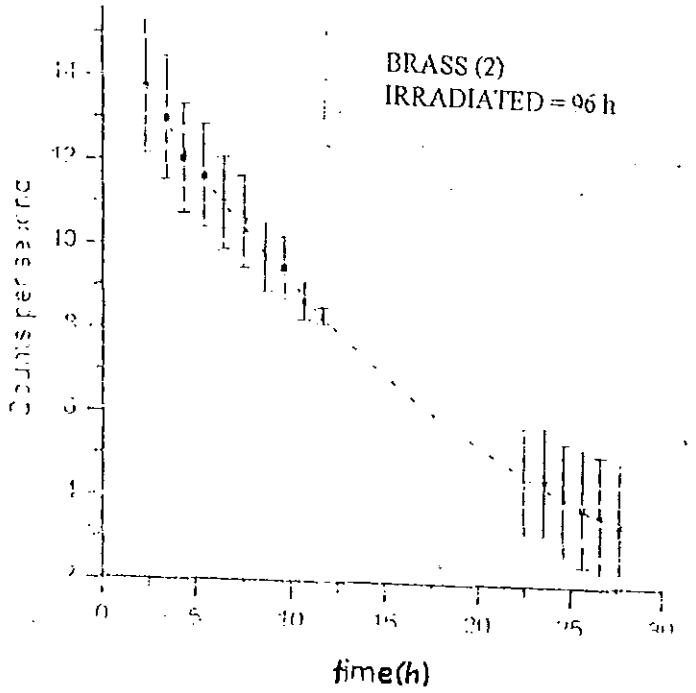

Fig. 6.9 Exponential decay of ^{64}Cu radionuclide in brass (2) sample

The experimentally determined half-life of ^{64}Cu when measuring the intensity of the 511 keV line is given in table 6.4.

Table 6.4 Experimentally determined half-life of ^{64}Cu using the 511 keV line

Sample	Decay constant (λ)	Half-life (h)	% of the t^* value
copper	0.05433	12.76	99.68
brass (1)	0.05255 +/- 0.00054	13.19 +/- 0.14	103.02
brass (2)	0.0543 +/- 0.00055	12.75 +/- 0.01	99.63
Average half-life of ^{64}Cu in brass is 12.97 +- 0.09h			

$t^*_{1/2}$ =12.8 h half- life of ^{64}Cu from literature [20]

The experimentally determined mean value half-life of copper-64 isotope was determined here was 12.97 +/- 0.09h..

CALCULATION OF ELEMENT CONCENTRATIONS

The second part of the experiment is to determine the concentration of copper within the brass samples. The amount of copper in brass was determined from the observed gamma-ray spectra by suitable comparison with corresponding spectra of activated pure copper by photopeak area method. The net area of the 511 keV photopeak is directly proportional to the absolute gamma emission rate of the corresponding copper-64 isotope. The spectrum we obtain after stripping is a single peak due spectrum to copper-64 at 511 keV as shown in Figs. 6.11, 6.12 and 6.13. This 511 keV peak representation is satisfactory since the peak to background ratio is small. The comparative method which is used to find the amount of copper in brass is given by the following relation

$$\text{Element mass in sample} = \text{Element mass in standard} \times \frac{\text{Number of counts in the sample}}{\text{Number of counts in the standard}} \qquad (3.5)$$

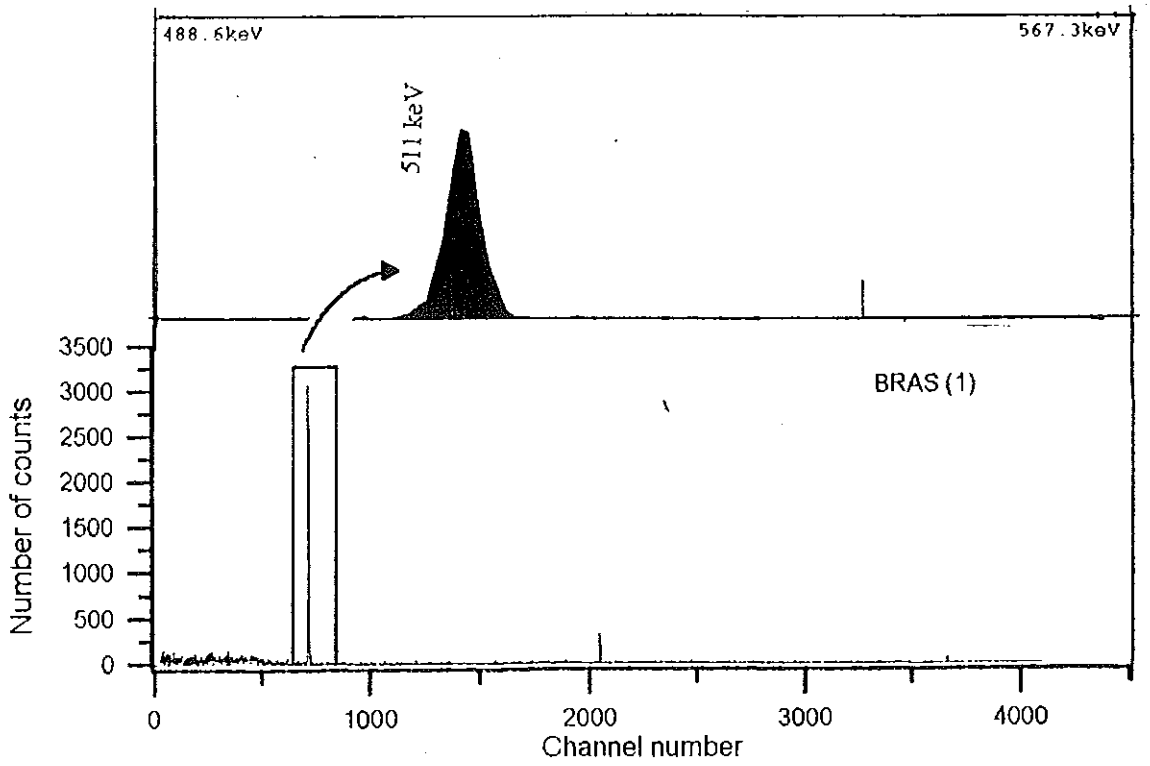

Fig. 6.11 Photopeak area of the 511 keV annihilation line in brass (1)

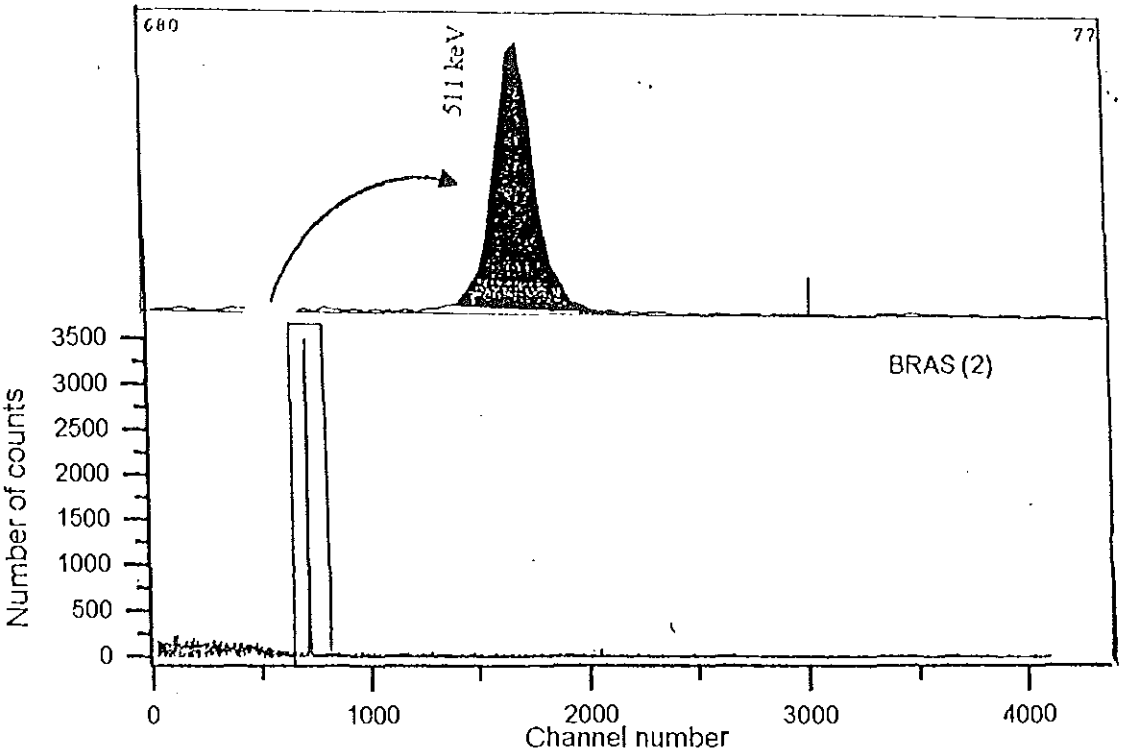

Fig. 6.12 Photopeak area of the 511 keV annihilation line in brass (2) sample

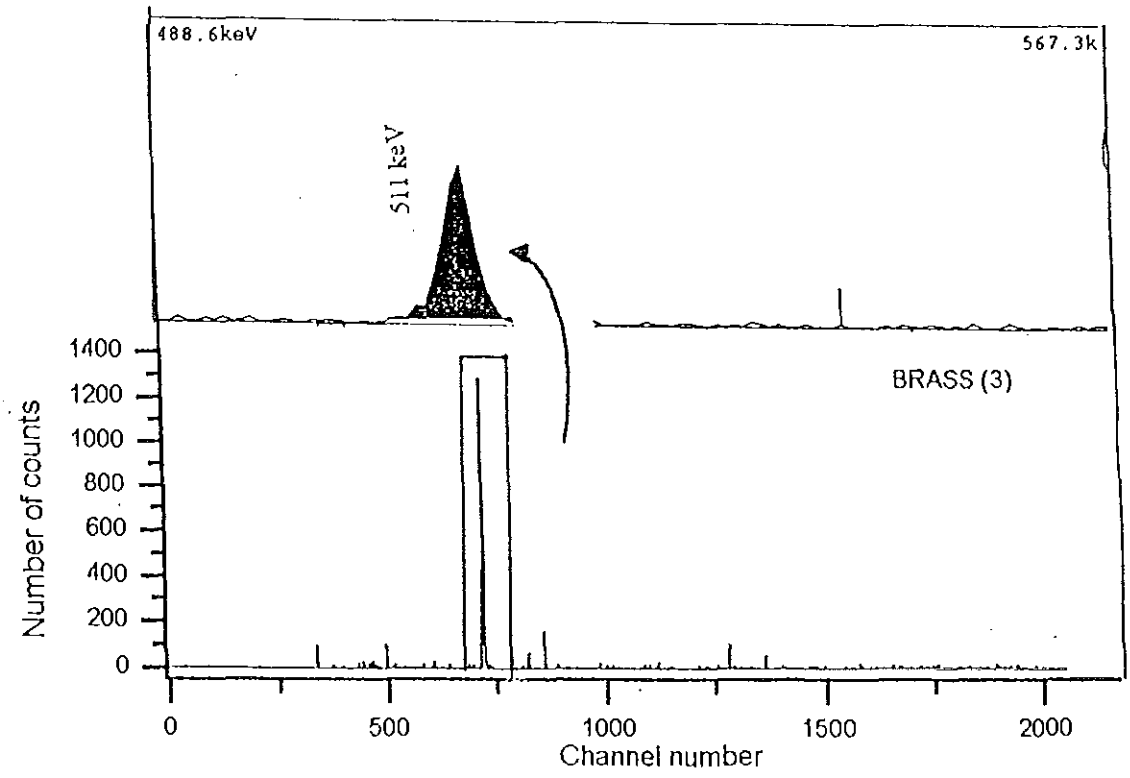

Fig. 6.13 Photopeak area of the annihilation line in brass (3)

Table 6.5 Measured amount of copper in brass samples

Sample Type	Area (counts)	Mass of the sample (g)	Mas of copper in the sample (g)	Percentage of Cu in the sample (%)
Standard Cu(1)	14777	2.18	2.18	100
Standard Cu(2)	14330	2.31	2.31	100
Standard Cu(4)	13945	2.35	2.35	100
Brass(1)	12501	3.35	2.11	62.99
Brass(2)	15027	3.55	2.53	71.27
Brass(3)	6440	1.50	1.09	72.67
			Average =	68.97%

Table 6.4 and 6.5 contain the results of NAA of copper and brass samples which have been randomly collected from different parts of Addis Ababa city. At present the brass is widely used in Merkato for decorative architecture. Because of this fact it was interesting to investigate the uniformity of copper within brass which is circulating in the market. Generally a brass sample is an alloy of copper and zinc which usually contains 70.8% of copper and 26.7% of zinc [21]. In order to determine the content of copper within the brass sample, the sample was prepared to have a good geometrical form, the required mass, and thickness (see table 5.5.). The experimental set up was used according to Fig. 4.4 in which the electronics part of the measuring system was arranged according to have good sensitivity. The energy calibration of the spectrometer was done using a standard radionuclide source containg ^{137}Cs, ^{134}Cs, ^{60}Co and ^{40}K (see appendix D). After the brass and the copper sample prepared, they were placed into an Am-Be neutron source irradiation channel. The sensitivity of the measurement depends upon both the intensity and duration of irradiation. Since our Am-Be neutron source does not have a high flux of neutrons, the optimum irradiation condition is based on the half-life of the nuclide under investigation (12.8h for ^{64}Cu). The half-life of copper is relatively short with respect to the

other activation product zinc. We irradiated the brass sample for longer time in order to minimise the gross activation of other trace elements within the brass which contribute to the spectrum and makes the analysis more complicated. In order to have measurable activity the brass and standard Cu samples were irradiated for different half-life (see table. 6.5). The nuclear reactions that take place between thermal neutrons and the brass sample are given in table 6.6

Table 6.6 Nuclear reactions between thermal neutrons and copper and zinc samples [22]

Reaction	Thermal neutron cross-section	Abundance of isotope(%)	Half-life of product	Principal gamma rays (keV)
$^{63}Cu(n,\gamma)^{64}Cu$	4.5 b	69.1	12.8 h	511, 1340
$^{63}Cu(n,p)^{63}Cu$	3.1 +- 0.5 mb	-	80 y	-
$^{65}Cu(n,\gamma)^{66}Cu$	2.2 b	30.9	5 min.	830, 1040
$^{64}Zn(n,\gamma)^{65}Zn$	0.44+- 0.5 mb	48.89	245 d	1190
$^{66}Zn(n.P)^{66}Zn$	20 μb	27.81	80 y	-

From the table we see that the ^{63}Cu (n , γ) ^{64}Cu reaction has a very large cross-section and the 511 keV gamma ray energy created after decay of copper-64 is a very convenient energy for detection with a Ge detector (see Fig. 6.12).

The ordinary copper consists of $69^{0}/_{0}$ copper-63 for which the neutron capture cross-section is 4.5 barn, and $31^{0}/_{0}$ copper-65 for which the cross-section is 2.2 barn. The relative neutron absorption is therefore proportional to 69x4.5 and 31x2.2, respectively, and we see that $82^{0}/_{0}$ of the neutrons absorbed by ^{63}Cu produce the nuclide we want, copper-64. Furthermore, copper-66, has a half-life of only 5 minutes, while copper-64 has a half-life of 12.8 h. Hence six hours after exposure of our brass sample, the copper-64 lost by decay only about $40^{0}/_{0}$ of its activity, while copper-66 decayed practically completely. Since the cross-section of the $^{63}Cu(n,\gamma)$ reaction is fairly large, a small piece of brass could be used to have good specific activity (see table 5.5).

The decay scheme of ^{64}Cu is represented in Fig. 5.2 . Main decay modes are the electron capture and the β^-- decay directly to the ground states of ^{64}Ni and ^{64}Zn, respectively. The 1346 keV line from the ^{64}Ni decay appears only with a small branching ratio (0.5%). Therefore, we used the β^+ decay of ^{64}Cu (branching ratio of 19%) to identify this nuclide. The positron annihilates with a electron in the sample. This way two annihilation gamma-ray photons of energy 0.511 keV each are created.

In the background spectrum (see Fig. 6.1) the following daughter activities are identified, ^{208}Tl, ^{212}Bi, from thorium series, ^{214}Bi, ^{210}Tl, from uranium series. As in all background measurements, also in our case the ^{40}K-line at 1460 keV is seen.

This background spectrum was stripped from the sample spectra. The main single dominant photopeak in the spectrum remained is the 511 keV line (see Fig. 6.11, 6.12, and 6.13). To make sure that this line in the spectrum is indeed the annihilation photopeak of ^{64}Cu, we have measured the half-life of 511 keV line by direct counting method.

DETERMINATION OF HALF-LIFE OF ^{64}Cu: This measurement was made from the gamma-ray spectra of the activated brass samples. The measurement of the half-life was done by taking the count of the 511 keV-line of the spectra from brass and copper.The measuring time for each individual spectrum was pre-set to be 1000 S. The count rate was measured almost every hour for 27 hours. Substituting the experimentally determined decay constant into Equ. 3, the half-life of ^{64}Cu obtained is 12.97 +/- 0.09 h (see table 6.4). This experimentally determined half-life deviate from the value in literature (12.8 h) only by 1.32%.

QUANTITATIVE ANALYSIS: To obtain information about the copper content in brass, we have used a comparative method utilising sample of copper which is irradiated simultaneously with the brass samples and assayed in the same manner. This technique of

relative measurements can be carried out easily and does not require absolute assay technique.

The amount of copper-64 activated in the brass sample was determined from the observed peak content of the 511 keV line in the brass and copper spectra, respectively. The area of the photopeak is given in table 5.5. The spectra of the standard copper and brass samples in Figure 6.11, 6.12, and 6.13 show that the peak occurred in flatter region of fairly constant response. The intermediate half-life of copper-64 implies this isotope have one relatively strong peak at 511 keV and a weak peak at 1346 keV. The total amount of copper in the brass samples is determined in table 6.5 (see analysis result), which is found to be 68.97% of the mass of brass. This experimentally determined amount of copper in the brass sample varies only by 2.59% from the value in literature which is 70.80%.

The results are shown in table 6.4 and 6.5. The major source of error in deducing the half-life and the amount of copper in brass arise from counting statistics and background subtraction. Several sources of counting error contribute to the variation of the experimental results. One of them is the statistical error. Analytical source of errors include surface contamination of the sample, introduction of contaminants during sample preparation and nuclear source of errors which include self-shielding for thermal neutrons in the sample, failure due to flux gradients during irradiation, interference from competing reactions and interference from primary or secondary reactions. In our case of ^{61}Cu only the statstical error contributes.Taking into consideration the error sources the obtained results are in good agreement with the expectations. This demonstrates the good reliability of neutron activation analysis for quantitative investigations of materials.

In the second part of the experiment the main objective of the experiment is to show that the NAA also works for other elements. Corresponding results are shown in Figs.5.8, 5.9 and 5.10.

Iodine in chemical compounds

An interesting element is iodine, e.g. in the enviroment, for food production. ^{128}I can be created in the $^{127}I(n, \gamma)$ reaction. The half-life of ^{128}I is 25 min. According to the decay scheme (see appendix C) at least the line at 443 keV could be expected. A test measurement with 1 g of pure I clearly shows this line, and even the lines at 527 keV and 970 keV with weak intensities are seen (see Fig. 5.8).

Thus, it was interesting to irradiate chemical compounds containg I. We selected two samples with KI and KIO_4 with 1.1 g and 0.51 g of I content, respectively. The 443 keV-line appears in both spectra clearly, and the quantitative content of 2:1 of I in KI and KIO_4 could be exactly reproduced.

Manganese in $KMnO_4$

The activation of ^{55}Mn (100% abundance) was tested in $^{55}Mn(n, \gamma)^{56}Mn$. The produced nuclide has a half-life of 2.58 h and a prominent line at 847 keV. We irradiated 2 g of $KMnO_4$ for only two half-lives, and measured the spectra after a cooling time of one half-life and again after six half-lives. As shown in Fig. 5.9 the Mn signal is seen clearly. This result is quite understandable. The 100% abundance is one of the facts, and the other one is the very large capture cross-section for thermal neutrons, which is of the order of several 10 b. In a thermal neutron field, the only spectral interference can come from the activity of ^{27}Mg, which has a line at 844 keV and, therefore, might interfere with the

Mn-line. A half-life study usually is done in such cases to identify the nuclide of interest. Here this procedure is not necessary, because Mg generally occurs in small concentrations when analysing e.g. ore samples. Besides the capture cross section for thermal neutrons is small and the half-life of ^{27}Mg produced in the ^{26}Mg(n,γ) reaction is only 9.5 min.

Nickel sample

In natural nickel there are 6 isotopes, the one with the smallest abundance is ^{64}Ni. Its isotope mole fraction is only 0.91%. If (n,γ) activation carried out using natural Ni, one should look for the gamma-lines at 1116 keV and 1482 keV of ^{65}Ni. The half-life of this nuclide is 2.52 h.

A Ni sphere was irradiated for about 20 h and then and again after a cooling time of two $t_{1/2}$ the gamma- spectrum measured. We looks for the 1116 keV-line, and no indication of the appearance of ^{65}Ni was seen at the first glance. At this energy one should be careful, as there is a rather strong background line at 1120 keV belonging to ^{214}Bi.

The "negative" result is quite understandable. The total cross-section for thermal neutrons on natural Ni is 23.1 b, 80% elastic and 20% (n,γ). At higher energies (e.g. 1MeV) this situation becomes even worse, the total cross section is 3.7 b, with elastic scattering more than 99%. For (n, γ) only 0.2% can be expected [23].

Nevertheless, the careful analysis shows, using the expand-mode of spectra representation of the S100-system that an indication of the low-abundant ^{64}Ni might be present. Possibly the Ni- signal interfer with some unknown nuclide. To clear up this result, further quantitative analysis is necessary, which goes beyond this work.

CONCLUSION

Neutron irradiation for activation analysis using the isotopic ^{241}Am-Be neutron source has shown remarkably good induced radioactivity for ^{64}Cu, ^{128}I, ^{56}Mn and ^{65}Ni . In this work the half-life of copper-64 has been found to be 12.97 +/- 0.09 h. This result is comparable with the exact value (12.8 h), which confirms that the 511 keV line is the annihilation line of ^{64}Cu. The concentration of copper in brass was determined, which was found, to be 68.90 % , in a good agreement with those values in literature.

Through the activation of chemical compounds of KI, $KMnO_4$ and Nickel one is able to do qualitative identification of ^{128}I, ^{56}Mn and ^{65}Ni. This result shows that using ^{241}Am-Be neutron source NAA is a good nuclear method for further research purpose and it is a reliable method for quantitative and qualitative analysis.

REFERENCES

[1] Koch, R.C., "Activation Analysis handbook", Academic press, Inc., Ltd., London (1960).

[2] Winchester, J.W., " Activation analysis in mineral prospecting", in: Proc. of panel on Nuclear techniques and mineral resources in developing countries, Vienna, Austria (1971).

[3] Mukhin, K.N., "Experimental Nuclear Physics Vol. 1", Mir Publ., Moscow (1987).

[4] Martin, Alan & Harbison, Samuel A., "An introduction to radiation protection", John wiley & sons, Inc., New York (1979).

[5] Boswell, G.G., & Fairs, R.A., " Radioisotope laboratory techniques", Butter Worth & Co., Ltd., Boston (1981)

[6] Friedlander, Gerhart & W.Kennedy, Joseph "Nuclear and radiochemistry", John Wiley & Sons, Inc., London (1960)

[7] Mukhin, K.N., " Experimental Nuclear Physics Vol. 2", Mir Publ., Moscow (1987)

[8] Carswell, D.J. " Introduction to Nuclear Chemistry ", Elsevier Publ. Comp., Inc., New York (1967)

[9] L` Annunziata, M.F., "Radionuclide tracers, their detection and measurement", Academic press, Inc., London (1987).

[10] Debertin, Klaus & Hemler, Richard G., " Gamma and X-ray spectrometry with semiconductor detectors", Elsevier Publ. Comp., Inc., New York (1988)

[11] Clark, George li., " Encyclopaedia of X-rays and gamma-rays", Reinhold Publ. Corp., New York (1963)

[12] Guinn, V.P. & Wagner, C.D., Analy. Chem. 25, No 1, 318 (1960)

[13] Boyed, G.E., Anal. Chem. 21, 335 (1949).

[14] Meink, W.W & Anderson, R.E, Anal. Chem. 25, 77 (1953)

[15] Valkovic, Vlado, "Nuclear microanalysis", Gerland Publ. Inc., New York (1977).

[16] Meink, W.W & De, A.K, Anal. Chem. 25, 778 (1958).

[17] Strain, J.E., & Lyon, W.S., "The use of isotopic neutron sources for chemical analysis", in Proc. of a Symp., Salzburg, 1964

[18] Meink, W.W & Anderson, R.E, Anal. Chem. 25, 77 (1953)

[19] Leddicotte, G.W., "Experience in the USA on the use of radioactivation analysis", in: Proc. of the Radioactivation analysis Symp. Vienna, Austria (1959).

[20] Nuclear data of copper-64, Technical reports series No. 63, IAEA, Vienna, 1966.

[21] Butts, Allison, " The science and technology of the metal, its alloy & compounds", Reinhold Publ. Corp., New York (1954).

[22] Bernard, G. Harvey, "Introduction to nuclear physics & chemistry", Prentice-Hall, Inc., New Jersey (1969).

[23] Neutron Induced Reaction cross-section data for nuclides required for Bore hole logging and mineral analysis, Technical reports No. 357, IAEA, Vienna 1993.

APPENDIX A

Detector specification and performance data of Ge detector

The coaxial Germanium detector which is used for measurement of photon energy have the following properties:

1.1. SPECIFICATIONS

- Relative efficiency ---------- $50^{0}/_{0}$
- Resolution ---------- 2 keV (FWHM) at 1.33 MeV
- Peak/compton ---------- 62 :1
- cryostat description----------U-style integral cryostat type 7915.30

1.2. PHYSICAL/PERFORMANCE DATA

- Geometry ---------- coaxial one open end, closed end facing window.
- Diameter ---------- 48 mm
- Length ---------- 34.5 mm
- Active area facing window ---------- 18.1 cm^2
- Distance from window ---------- 5 mm

1.3. ELECTRICAL CHARACTERISTICS

- Depletion voltage ---------- +3000 V
- Recommended bias voltage ---------- +3500 V
- Leakage current at recommended bias -------- 0.1mA
- Preamplifier test point voltage at recommended bias--------- -2.1 V

APPENDIX B

Information data of neutron source of ^{241}Am-Be

1. Activity : 2 Ci
2. Dimensions : ϕ30x30 mm
3. Location : Center of the neutron sheilding tank.
4. Surface dose rate :

On the surface of the neutron sheilding tank

16.8 μsv/h (max.)

At place 0.5 meter far from the tank

3.8 μsv h (max.)

The neutron sheilding tank is shown in Fig. 4.4

APPENDIX C

DECAY SCHEME OF ^{128}I, ^{56}Mn, and ^{65}Ni

1. Decay scheme of Iodine-128

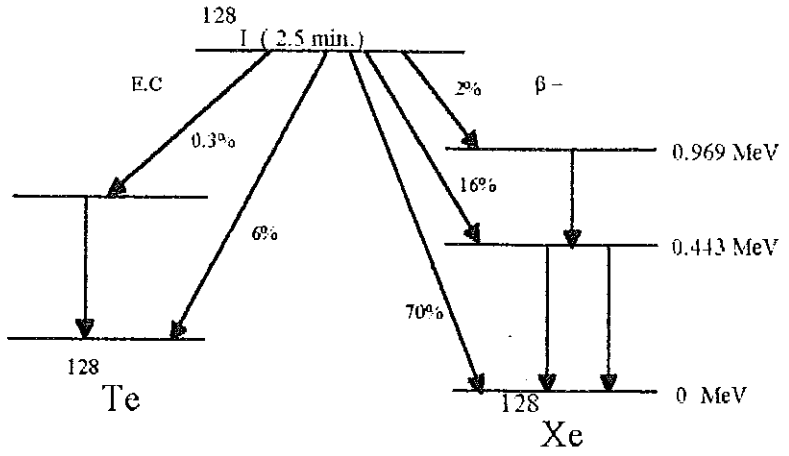

- mode of decay: β^- (93.1%) , E.C (6.9%)

- Production: $^{127}I(n, \gamma)$

- Main gamma energy: 442.91 keV (16.0%), 526.5 keV (1.57%), 969.4 keV (0.4%) ..

2. Decay scheme of manganese-56

- Decay: β^- (100%)

- Production: $^{55}Mn(n, \gamma)$

- Main gamma energy: 846.8 keV (98.9%), 1810.8 keV (27%), 2130kev (14.3%)..

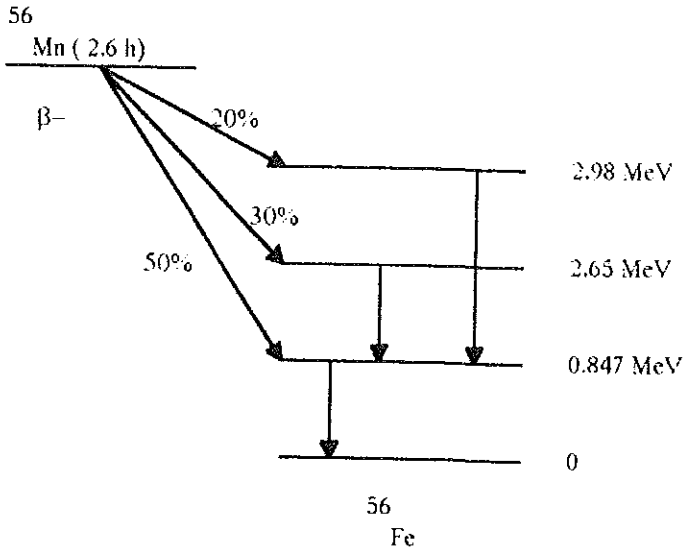

3. Decay scheme of nickel-65

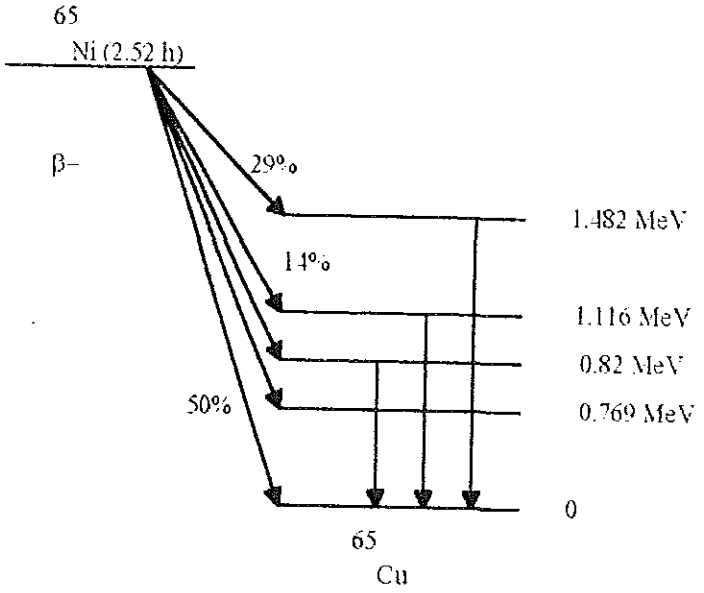

- Decay mode : β– (100%)

- Production : ^{64}Ni (n, γ)

- main gamma energy : 1.482 MeV (23.5%), 1.116 MeV (14.8%), 482 MeV (23.5%)

APPENDIX D

The standard samples that were used for energy calibration are:

Standard Radionuclide	Energy(keV)
^{137}Cs	661.66
^{134}Cs	604.67
^{40}K	1460.75
^{60}Co	1332.5

The equation of energy calibration is

$$E_\gamma = 4.72783 + 0.707659\# \text{ chan.} + 1.089 \times 10^{-6} \# (\text{chan.})^2$$